Published online 21 February 2019

Nucleic Acids Research, 2019, Vol. 47, No. 8 ***4255–4271***
doi: 10.1093/nar/gkz130

piRNA silencing contributes to interspecies hybrid sterility and reproductive isolation in *Drosophila melanogaster*

Alexei A. Kotov[1], Vladimir E. Adashev[1], Baira K. Godneeva[1], Maria Ninova[2], Aleksei S. Shatskikh[1], Sergei S. Bazylev[1], Alexei A. Aravin[1,2,*] and Ludmila V. Olenina[1,*]

[1]Institute of Molecular Genetics, Russian Academy of Sciences, Kurchatov Sq. 2, Moscow, 123182 Russia and [2]California Institute of Technology, Division of Biology and Biological Engineering, 147–75, 1200 E. California Blvd., Pasadena, CA 91125, USA

Received October 01, 2018; Revised February 12, 2019; Editorial Decision February 14, 2019; Accepted February 16, 2019

ABSTRACT

The piRNA pathway is an adaptive mechanism that maintains genome stability by repression of selfish genomic elements. In the male germline of *Drosophila melanogaster* repression of *Stellate* genes by piRNAs generated from *Supressor of Stellate* (*Su(Ste)*) locus is required for male fertility, but both *Su(Ste)* piRNAs and their targets are absent in other *Drosophila* species. We found that *D. melanogaster* genome contains multiple X-linked non-coding genomic repeats that have sequence similarity to the protein-coding host gene *vasa*. In the male germline, these *vasa*-related *AT-chX* repeats produce abundant piRNAs that are antisense to *vasa*; however, *vasa* mRNA escapes silencing due to imperfect complementarity to *AT-chX* piRNAs. Unexpectedly, we discovered *AT-chX* piRNAs target *vasa* of *Drosophila mauritiana* in the testes of interspecies hybrids. In the majority of hybrid flies, the testes were strongly reduced in size and germline content. A minority of hybrids maintained wild-type array of premeiotic germ cells in the testes, but in them harmful *Stellate* genes were derepressed due to the absence of *Su(Ste)* piRNAs, and meiotic failures were observed. Thus, the piRNA pathway contributes to reproductive isolation between *D. melanogaster* and closely related species, causing hybrid male sterility via misregulation of two different host protein factors.

INTRODUCTION

The maintenance of gametogenesis in heterosexual organisms is crucial for species viability and for the transfer of genetic information from generation to generation. Gametogenesis is often disrupted in the progeny of interspecies crosses. Indeed, hybrid male sterility has been proposed to be the dominant type of postzygotic interspecies isolation in *Drosophila* (1,2); however, the underlying mechanistic causes and factors involved are poorly understood. Germ cell proliferation and differentiation and genome integrity are under control of a number of mechanisms. One of conserved pathways required for gametogenesis and fertility in Metazoa is the Piwi-interacting RNA (piRNA) pathway; via this pathway small piRNAs of 23–29 nucleotides (nts) guide sequence-specific recognition and repression of complementary RNA targets (3,4).

In the *Drosophila* female germline, a diverse set of piRNAs represses the activity of mobile elements thus ensuring genome integrity. Failure of piRNA silencing that causes derepression of transposable elements and is associated with accumulation of double-stranded DNA breaks likely caused by transposons integrations and activation of the DNA damage check-point (5,6). Even when the DNA damage pathway is non-functional due to a mutation in Chk2 kinase, females with mutations that disrupt the piRNA pathway are sterile. Complex mechanisms are responsible for generation of diverse piRNAs that guide repression of mobile elements. Many piRNAs are generated from piRNA clusters, genomic regions that contain numerous fragments of transposons. piRNA clusters are transcribed—often from both genomic strands—to generate long non-coding RNAs that serve as precursors for mature piRNAs (3,4,7). After processing of precursors by Zucchini endonuclease, mature piRNAs, which usually contain a strong bias for uridine residue at the 5′-end (1U), are loaded into Piwi proteins (8,9). The recognition of complementary targets such as transposon mRNAs by the Piwi/piRNA complex leads to cleavage of the target RNA by the intrinsic endonuclease activity of Piwi proteins. In

*To whom correspondence should be addressed. Tel: +7 499 196 0809; Email: olenina_ludmila@mail.ru
Correspondence may also be addressed to Alexei A. Aravin. Tel: +7 499 196 0015, +1 626 395 4297; Email: aaa@caltech.edu

addition to the RNAi pathway, which causes complete target degradation, the ping-pong mechanism generates new, so-called secondary, piRNAs from processed target. Secondary piRNAs generated through ping-pong have a strong bias for adenine at position 10, 10A (7,10). Thus, generation of secondary piRNAs provides a clear sign of RNAs targeted by piRNA pathway. The feed-forward mechanism of the ping-pong cycle is believed to amplify piRNAs that target active transposons thus fine-tuning piRNA populations to meet cellular needs.

Several studies have reported that in *Drosophila*, piRNAs can also control the expression of host protein-coding genes. For example, piRNAs derived from the 3′ untranslated region (3′-UTR) of the *tj* gene repress the *fasciclin III* gene in follicle cells of the *Drosophila* ovary (11), while piRNAs from the *AT-chX* locus target *vasa* mRNA in germ cells of the testes (12,13). The piRNA-dependent decay of numerous maternal mRNAs occurs during the maternal-to-zygotic transition in early embryos (14), and piRNA-mediated repression of differentiation factor Cbl is involved in the self-renewal of germline stem cells (15). The piRNA pathway is also reported to control the maintenance and differentiation of germline stem cells through regulation of *c-Fos* mRNA in somatic niche cells (16). In most of these cases, piRNAs are reported to have only a partial complementarity to the proposed targets. The rules that govern the recognition of proper targets and discriminate against off-target effects are not clearly understood. Importantly, one study suggested that piRNA/Piwi complexes are able to target numerous cellular mRNAs in a nonsequence-specific manner (17).

While the majority of studies of the piRNA pathway in *Drosophila* were focused on the female germline, the piRNA pathway is also active in the testes. In fact, piRNA silencing was first demonstrated in testes (18–20). The major source of piRNAs in the testes is the Y-linked *Supressor of Stellate* (*Su(Ste)*) locus that produces piRNAs that target X-linked repetitive *Stellate* genes. Each *Stellate* repeat encodes a protein with a homology to the regulatory subunit of protein kinase CkII; however, *Stellates* are not expressed in wild-type males (21–23). Derepression of *Stellates* due to deletion of the *Su(Ste)* locus or failure of the piRNA pathway leads to accumulation of needle-like crystals of Stellate protein in spermatocytes, severe meiotic defects and sterility (21,23–25). Thus, *Stellate* and *Su(Ste)* loci, which are present in the genome of *Drosophila melanogaster* but absent in other *Drosophila* species, resembles selfish toxin/anti-toxin systems. Another unusual source of piRNAs in the testes is the *AT-chX* locus. It is located in the pericentromeric region of the X-chromosome and is reported to generate two distinct piRNAs that are complementary to coding sequence of *vasa* gene (12,13). In contrast to *Stellate*, *vasa* is an evolutionarily conserved host gene, and the function of Vasa protein is essential for proper gametogenesis in both sexes of *Drosophila* (26,27).

Here we investigated piRNA silencing in the testes of *D. melanogaster* and of interspecies hybrids between *Drosophila melanogaster* and *Drosophila mauritiana*. Genomic analysis showed that X-linked locus in cytolocation 20B is composed of at least 26 divergent *vasa*-related *AT-chX* repeats that are present in the genome of *D. melanogaster* but that are absent from the genomes of closely related *Drosophila* species. The *AT-chX* repeats have homology to the fourth and fifth exons of *vasa*, they are expressed from both genomic strands in developing spermatocytes, and they produce abundant piRNAs. However, we found no evidence that *AT-chX* piRNAs, which have ∼76% identity to *vasa* sequence, are able to repress *vasa* expression in the testes of *D. melanogaster*. In contrast, *AT-chX* piRNAs produced from the *D. melanogaster* genome have ∼90% identify with the *vasa* allele of *D. mauritiana* and selectively silence its expression in the testes of interspecies hybrids. The majority of hybrid testes maintain a few germ cells and are strongly reduced in size compared to parent flies. We also found a strong derepression of *Stellate* genes in the minor cohort of hybrid testes with perfect germline content that lacks the *Su(Ste)* locus. Overall, our results suggest that piRNA and mRNA sequences are fine-tuned to each other in each species to ensure silencing of proper targets and to avoid inappropriate repression. Accordingly, the piRNA pathway contributes to the reproductive isolation of *D. melanogaster* from closely related species via dysregulation of at least two different protein factors.

MATERIALS AND METHODS

Fly stocks

Germinal tissues of adult *Drosophila* males and females raised at 23°C were used, unless otherwise indicated. The $Df(1)w^{67c23(2)}y$ (designated as *yw*), *Oregon R, Canton S* and *Batumi L* strains were used as wild-type strains of *D. melanogaster*. Strains carrying *spindle-E (spn-E)* mutations were $ru^1\ st^1\ spn\text{-}E^1\ e^1\ ca^1/TM3$, $Sb^1\ e^s\ spn\text{-}E^1$, and $ru^1\ st^1\ spn\text{-}E^{hls3987}\ e^1\ ca^1/TM3,\ Sb^1\ e^s$. *aub* mutants were aub^{QC42}/CyO and aub^{HN2}/CyO. We also used a $piwi^2/piwi^3$ heteroallelic combination. Heterozygous siblings (+/−) were used as wild-type controls because they have closely related genetic background to flies carrying heteroallelic mutation combinations.

Drosophila sechellia, Drosophila mauritiana and *Drosophila erecta* stocks were obtained from the Gif-sur-Yvette CNRS Center (France) collection. *Drosophila simulans* stock w.501 was obtained from UC San Diego Drosophila Species Stock Center. The Hmr^1 strain of *D. melanogaster* (#2481) was obtained from Bloomington Drosophila Stock Center. *Drosophila simulans* stock C167.4 (#14021-0251.199) was obtained from UC San Diego Drosophila Species Stock Center.

Interspecies crosses of Hmr^1 *D. melanogaster* females with *D. mauritiana* (CNRS Center (France) males or with *D. simulans* (C167.4) males were performed at 21°C, and F1 progeny were collected.

Alignments of *AT-chX* repeats and *vasa* genes

Multiple alignments were performed using the Clustal W algorithm with subsequent manual adjustment. DNA sequences corresponding to heterochromatic *AT-chX* repeats were identified and collected using BLAT software associated with the *D. melanogaster* genome assembly *dm6* (UCSC Genome Browser, http://genome.ucsc.edu/). *vasa* sequences from different *Drosophila* species (GD23992 of

D. simulans; GM15916 of *D. sechellia*; GG25145 of *D. erecta*; GE20836 of *D. yakuba*; GJ11891 of *D. virilis*; GF14338 *of D. ananassae*) were retrieved from GenBank (NCBI) into Vector NTI 10 software (Invitrogen). The sequence of the *D. mauritiana vasa* gene was retrieved from the genome release 1.0 of the MS17 strain (http://www.popoolation.at/mauritiana_genome/) (28). The starts and ends of corresponding *vasa* exons of *D. mauritiana* were determined using conservative flanking sequences of splice site regions. For alignment with the *AT-chX* consensus, we used antisense *vasa* strands.

RNA library preparation

Small RNAs of 18–29 nt in size from the testes of *yw* and *Hmr[1] D. melanogaster*, *D. mauritiana*, and interspecies hybrids were cloned as previously described in (7,29). The libraries were barcoded according to Illumina TrueSeq Small RNA sample prep kit instructions and sequenced using Illumina HiSeq-2500 or HiSeq-4000 sequencing systems (50-bp runs). For the preparation of RNA-seq libraries testis, RNA was isolated from *D. melanogaster*, *D. mauritiana* and interspecies hybrids with TRIzol Reagent (Invitrogen). rRNA was depleted with Illumina Ribo-zero rRNA removal kit (Human/mouse/rat). Standard RNA-seq libraries were generated using the NEBNext Ultra™ II Directional RNA Library Prep Kit for Illumina (#E7760, NEB) according to the manufacturer's instructions and sequenced on the Illumina HiSeq 2500 platform (50-bp runs).

Bioinformatics analysis

Adapter sequences used in small RNA and total RNA-seq library sequencing were removed using cutadapt 1.8.1. For analysis, small RNA reads from the *yw* library were passed through quality control and minimal length (>18 nt) filter and were finally mapped to genome of *D. melanogaster* (*dm6* assembly, UCSC Genome Browser, https://genome-euro.ucsc.edu/cgi-bin/hgGateway?redirect=manual&source=genome.ucsc.edu) without mismatches (0 mm) using bowtie 1.2.2. Length distribution plot was calculated for mapped reads. Small RNAs that mapped to the *dm6* genome assembly without mismatches according the coordinates of the *AT-chX* repeats were used for the calculation of length distribution and sense/antisense ratio. For graphical read distribution analyses, small RNAs were mapped to consensus of *AT-chX* repeats allowing 0–1 mismatch (mm). Sequence logos were generated with the WebLogo application (30). The ping-pong signature was defined as normalized occurrence frequencies of overlap lengths between the 5′-ends of small RNAs mapped to the opposite strands using signature.py script (31). For substitution frequency analysis at each nucleotide position, the small RNA library from *yw* flies was mapped to *vasa* and *Stellate* sequences with 0–3 mismatches allowed. The numbers of mismatches at different positions were calculated. The consensus *Su(Ste)* sequence was used for mapping of small RNAs to the *Su(Ste)* repeats. Length distribution, sense/antisense ratio and graphical distribution of reads were calculated for mapped reads allowing 0–1 mm.

For analysis of small RNA reads (>15 nt) from interspecies hybrids, the libraries were mapped to the *D. melanogaster* (*dm6* assembly) and *D. mauritiana* (release 1.0 of MS17 strain, http://www.popoolation.at/mauritiana_genome/) (28) genomes using bowtie 0.12.7. For specific analysis of piRNA production from the *AT-chX* repeats, small RNAs (23–29 nt) mapped to genome coordinates corresponding to the *AT-chX* repeats were reported. Sequences aligned with each individual repeat were counted. piRNAs were mapped to *vasa* genes of both parental species and to *AT-chX* repeat consensus sequences without mismatches, and mapped reads were also counted. Comparative analysis of piRNAs mapped to transposons in the testes of hybrid males was performed using coordinates of transposable element sequences (UCSC repeat masker track).

For specific analysis of *AT-chX* repeat expression, total RNA-seq reads from interspecies hybrid libraries were first aligned to the sequences of the 26 repeats allowing no mismatches and reporting all perfect alignments using bowtie 0.12.7. Reads mapped to *AT-chX* repeats were then mapped to the *D. melanogaster* (excluding the 26 *AT-chX* repeat regions) and *D. mauritiana* genomes, and the numbers of mapped positions within and outside of the 26 *AT-chX* repeats were calculated. The expression levels of sense and antisense long *AT-chX* mRNA transcripts were inferred based on reads that mapped exclusively to the *AT-chX* loci. For specific analysis of *D. melanogaster* and *D. mauritiana vasa* expression, total reads were first aligned to the *vasa* genomic sequence of the two species allowing no mismatches and reporting all perfect alignments using bowtie 0.12.7. The *vasa*-mapped reads were then mapped to the complete genomes of the two species with the *vasa* regions excluded. The reads were classified as unique to *vasa* in each species or non-unique (aligning to both *vasa* and other loci). Reads that uniquely mapped to the *vasa* exonic regions in either *D. mauritiana* or *D. melanogaster* were used for *vasa* expression analysis.

All data were normalized as reads per million (rpm) or reads per kilobase per million (rpkm). Read counts corresponding to regions of interest and downstream analyses were performed using BEDtools (32), SAMtools (33), and custom Bash and Python scripts available upon request. Supplementary Table S1 contains short descriptions of RNA libraries that were prepared and analyzed in this study. GEO accession number for the library data is GSE120802.

PCR analysis

For identification of the *AT-chX* repeats present in different strains of *D. melanogaster*, polymerase chain reaction (PCR) analysis of genomic DNAs was performed with primers to the repeats shown below. Genomic DNA was isolated from 10 to 20 flies using Wizard Genomic DNA Purification Kit (Promega) according to the manufacturer's instructions. Amplified DNA samples were separated by electrophoresis in a 1% agarose gel and visualized with ethidium bromide.

For RT-PCR analysis, total RNA was isolated from 50 to 100 pairs of dissected testes using TRIzol Reagent (Invitro-

gen). Complementary DNA (cDNA) was synthesized using random hexamers and SuperScriptII reverse transcriptase (Invitrogen). cDNA samples were analyzed by PCR or real-time quantitative PCR using incorporation of SYTO-13 (Invitrogen). All experiments were performed with at least three independent RNA samples; each sample was analyzed in duplicate. Statistical analysis for the group comparison was performed by a paired Student's *t*-test.

The following primers were used for PCR or RT-PCR: *rp49* fw 5′-ATGACCATCCGCCCAGCATAC-3′, rev 5′-GCTTAGCATATCGATCCGACTGG-3′; *vasa* of *D. melanogaster* fifth exon fw 5′-TTGGAAGACCCCAG GTAGTG-3′, rev 5′-CGATCCACGAAATCCAGAAG-3′; *solo* fifth exon fw 5′-CCTCCAGCATCAACACCTTT-3′, rev 5′-CGGGAAAGCAACACTCATTT-3′; *vig* second exon fw 5′-CTGTCCTTGACCGCTACCA-3′, rev 5′-GC CAGCAGCAATTACAAACA-3′; *Stellate* fw 5′-ATCGAT TGGTTCCTCGGGATCAA-3′, rev 5′-GCCGTACAAC AAGCCAGAGGAACTA-3′; *AT-chX* fw 5′-AGCGATCC CACTGCTAAAGA-3′, rev 5′-GTCGAAGACGTCCA GAGGAG-3′; *vasa* of *D. mauritiana* fw 5′-TCAGCAAATT GTTAGATGATCCTCAAGAT-3′, rev 5′-CTTCAAAC GTGACAAAAGCCCGA-3′; *aub* of *D. melanogaster* fw 5′-TGGGTCCCTCGATAGAGAAATCC-3′, rev 5′-CCAC TCCTTTCTTGCTGGTCATC-3′; *aub* of *D. mauritiana* fw 5′-CTCAAGTGGTTCCCTCGATGAG-3′, rev 5′-ACGG TAATATGAGTGCCCACCA-3′. We used *rp49* (*rpL32*) as a loading control.

In situ hybridization

The dissected testes of adult males were fixed in 3.7% formaldehyde in 1× phosphate buffered saline (PBS) with 0.1% Tween 20 (PBT). Then fixed tested were rinsed three times with PBT. Permeabilization of testes was performed by incubation in PBT with 0.3% TritonX-100 and 0.3% sodium deoxycholate solution for 1 h at room temperature (RT). A DNA template (446 nt) was synthesized for the generation of RNA probes by PCR of genomic DNA from wild-type flies using following primers that contain T7 promoter sites: 5′-AGCGATCCCACTGCTAAAGA-3′ and 5′-TAATACGACTCACTATAGGGATAAAAGG TGACCGGCAACG-3′ for detection transcripts from positive (antisense) strand and 5′-TAATACGACTCACT ATAGGGAGCGATCCCACTGCTAAAGA-3′ and 5′-ATAAAAGGTGACCGGCAACG-3′ for detection transcripts from negative (sense) strand. Digoxigenin-labeled RNA probes were synthesized using the MEGAscript T7 Kit (Ambion) and DIG Labeling mix (Roche). For pre-hybridization, the testes were incubated in a solution of 50% formamide in 750 mM sodium chloride and 75 mM trisodium citrate, pH 7.0 (HYB buffer) and PBT (1:1 ratio) for 10 min with rotation. Then testes were incubated in HYB buffer (HYB-) and HYB buffer with 0.5 mg/ml yeast RNA and 0.2 mg/ml heparin (HYB+) during 10 min. Hybridization was performed in HYB+ with RNA probes for 1 h at 42°C. After hybridization, testes were rinsed twice with HYB-, once with HYB-/PBT (1:1) for 20 min at 42°C and four times with PBT for 20 min at RT with rotation. Then immunostaining was performed as described previously in (34) starting from blocking stage.

Immunofluorescence staining and confocal microscopy

Testes of adult flies were dissected in cold PBT (PBS with 0.1% Tween20), washed once with PBT and fixed in 3.7% formaldehyde in PBT. All the following procedures were carried out as described previously (34). Staining was detected by laser scanning confocal microscopy using a Carl Zeiss LSM 510 META machine (Carl Zeiss) in multichannel mode with 40× oil objective (Numerical Aperture 1.4), frame size 1024 × 1024 pixels, scan speed 7, with four repetitions. All images were taken with the *z*-resolution of 1 μm. The obtained images were imported into Imaris®5.0.1 (BitplaneAG) for subsequent processing.

Antibodies

The following antibodies were used for immunofluorescence staining:

A mix of murine monoclonal anti-lamin Dm0 ADL67.10 and ADL84 antibodies (Developmental Studies Hybridoma Bank (DSHB), University of Iowa), 1:500; guinea pig monoclonal anti-Traffic jam (Tj) antibody (35), 1:5000; rabbit polyclonal anti-Vasa antibodies (a gift from Dr R. Lehmann),1:5000; rat monoclonal anti-Vasa antibody (DSHB), 1:100; murine polyclonal anti-Stellate antibodies (25), 1:250.

AlexaFluor 488 goat anti-rat IgG, Alexa Fluor 546 goat anti-rabbit IgG and Alexa Fluor 647 goat anti-mouse IgG (all from Invitrogen) were used as secondary reagents at a dilution of 1:500. 4′,6-diamidino-2-phenylindole (DAPI) was used for chromatin staining.

For western blot analysis, the following antibodies were used:

Murine monoclonal anti-actin ab8224 antibody (Abcam), 1:4000; rat monoclonal anti-Vasa antibody (DSHB), 1:4000; rabbit polyclonal anti-VIG/VIG2 antibodies 1803 (36), 1:500; murine monoclonal anti-AGO3 9G3 antibody (10), 1:250; murine monoclonal anti-Aub 4D10 antibody (12), 1:500.

Alkaline-phosphatase-conjugated anti-mouse, anti-rabbit and anti-rat antibodies (Sigma) were used as secondary reagents at a dilution of 1:20 000. Samples were resolved by sodium dodecyl sulphate-polyacrylamide gel electrophoresis and blotted onto Immobilon-P PVDF membrane (Millipore). Blots were developed using the Immun-Star AP detection system (Bio-Rad Laboratories) in accordance with the recommendations of the manufacturer. All experiments were performed at least in triplicate with independent preparations of testis and ovarian lysates. For densitometry analysis, ImageJ free software was used (https://imagej.nih.gov/ij/).

RESULTS

Genomic distribution and structure of *AT-chX* repeats

Previous studies described pericentromeric *AT-chX* locus as a source of two distinct piRNAs that target and repress *vasa* mRNA (12,13). To comprehensively identify the genomic sources of piRNAs that might regulate *vasa* expression, we used the sequence of *vasa* gene to query the *dm6* assembly of *D. melanogaster* genome. In addition to *vasa* gene located on the chromosome 2, we found 26 fragments that

have common organization and harbor sequences that are similar to the whole fourth and part of the fifth *vasa* exons. Two shorter fragments with lengths of 274 and 156 bp were described previously as the *AT-chX* regions (12). We designate whole set as *AT-chX* repeats. All 26 *AT-chX* repeats are located within a 553-kb region in the pericentromeric heterochromatin of the X chromosome (in cytolocation 20B with the exception of repeat #26, which is located in 20C) and have the same genomic orientation (Supplementary Table S2 and Figure 1A). We did not find sequences related to other *vasa* exons or *vasa* introns in this region or elsewhere in the genome assembly. The region of the X chromosome that harbors the repeats contains a few protein-coding genes, and multiple sequences that correspond to transposable elements and simple repeats. The *AT-chX* locus is located 28-kb downstream of the piRNA cluster *flamenco* that generates piRNAs in ovarian follicle cells (Figure 1A).

Careful examination of the *AT-chX* repeat sequences revealed that individual repeats have different internal organization (Figure 1B). The majority of the repeats (24 out of 26) are flanked by fragments of the transposable element *baggins1* (Supplementary Table S2 and Figure 1B). Many repeats also contain internal insertions of other mobile elements, such as *TIRANT* and *DM297*, and a genomic repeat sequence of unknown origin (*gr*), which break the continuity of the sequence homologous to *vasa* (Figure 1B and Supplementary Figure S1). Whereas all repeats contain a sequence similar to the fourth exon of *vasa* (*vasa-related-exon 4*, *Vr-ex4*), the length of this sequence varies from 107 to 251 nt. Furthermore, in addition to this sequence, the majority of the repeats also contain 23–159 nt homologous to the 5′-end fragment of the fifth exon of *vasa* (*vasa-related-exon 5*, *Vr-ex5*). Surprisingly, the *Vr-ex4* and *Vr-ex5* sequences are arranged in the repeats in reverse order compared to their arrangement in *vasa* gene (Figure 1B). Multiple sequence alignment of the repeats showed that they have a high level of sequence similarity to each other (Figure 1C and Supplementary Figure S1). Pairwise sequence comparison revealed that with the exception of one divergent sequence (repeat #17) *AT-chX* repeats can be divided into two distinct groups. Group 1 consists of repeats 1–4, 6–8, 10–16, and the group 2 consists of repeats 5, 9, 18–26 (Figure 1C). Interestingly, most of the repeats that belong to each group are clustered together in the genome (Figure 1A). *AT-chX* repeats have extremely high intragroup similarity: the levels of sequence identity are 99.0–100% for the first group and 96.9–99.5% for the second group. Between the two groups, the sequence identity is 90.6–95.6%. Thus, *AT-chX* repeats are more similar within group than between groups. The *AT-chX* repeats have on average only 76.4% identity to corresponding sequences of *D. melanogaster vasa* gene (Figure 1C and Supplementary Table S3). Overall, comprehensive analysis revealed a high level of sequence similarity between the *AT-chX* repeats, and, at the same time, high complexity of their internal organization.

To explore if *AT-chX* repeats are present in different strains of *D. melanogaster*, we performed PCR with primers designed to amplify 23 of 26 the repeats found in the reference genome assembly *dm6* using genomic DNA of *Oregon R, Canton S, Batumi L* and *yw* strains. We detected PCR fragments of three different lengths (274, 439–445 and 895–907 bp) that match the lengths expected from amplification of 22 repeats from both groups identified in the reference genome (Figure 1D and Supplementary Figure S2). This result indicates that the *AT-chX* repeats are conserved in different *D. melanogaster* strains. Next, we explored conservation of the repeats in other species of *Drosophila*. PCR analysis of genomic DNA from *D. sechellia, D. simulans* and *D. erecta* did not reveal PCR fragments corresponding to the repeats (Figure 1D). A bioinformatics search for *vasa*-related sequences using BLAST and BLAT software in the genome assemblies of several species presented on UCSC Genome Browser (*D. erecta, D. yakuba, D. ananassae, D. virilis*, *D. sechellia*, and *D. simulans*, the latter two are closest to *D. melanogaster*) did not reveal the presence of *AT-chX*-like repeats in the genomes of these species. Furthermore, analyses of the *D. yakuba* genome assembly using *vasa* sequences of *D. melanogaster, D. simulans, D. sechellia, D. erecta* and *D. yakuba* as queries also did not reveal any traces of *AT-chX*-like repeats. We assume that the repeats did not exist in the last common ancestor of the *D. melanogaster* subgroup but rather emerged later in evolution and then lost in closely related species. Thus, the *AT-chX* repeats are absent in the genomes of other *Drosophila* species, at least in the form present in *D. melanogaster* genome.

Expression of *AT-chX* repeats in developing spermatocytes

To study the expression of the *AT-chX* repeats, we cloned and sequenced a library of long RNAs (depleted of rRNA) isolated from dissected testes. Analysis of the RNA-seq library revealed that both strands of the *AT-chX* repeats are expressed in the testes at a very low level (0.45 rpkm). We also detected transcripts of different *AT-chX* repeats by RT-PCR analysis in the testes of *yw* males (Supplementary Figure S2).

To further examine the pattern of the repeat expression in the testes, we performed strand-specific RNA FISH of whole-mount testes preparations using *AT-chX*-specific probes. In the fly testis, germ cells at different stages of spermatogenesis are surrounded by somatic cyst cells and are arranged along the long axis of testis with germline stem cells positioned at the apical tip and cells corresponding to later stages further away from the tip (Figure 2A). Transcripts from both genomic strands of the *AT-chX* repeats were detected in Vasa-positive germ cells, but not in Tj-positive somatic cyst cells (Figure 2B). Transcripts of the *AT-chX* repeats that were antisense relative to *vasa* mRNA and transcripts sense to the *vasa* mRNA were present in a relatively narrow area close to the apical tip that corresponds to early spermatocytes in S phase and early G2 phase (Figure 2B and C). These transcripts were absent from germline stem cells in early stages of development and from mature spermatocytes, whereas *vasa* gene is known to be expressed in all premeiotic germ cells of the testes (26). The signal intensity of FISH confirmed the results of RNA-seq and indicated that antisense transcripts are more abundant than sense ones. *AT-chX* repeat transcripts detected by FISH were localized exclusively in the nuclei of germ cells: at the peak of their expression the abundant antisense transcripts occupied a large fraction of the nuclear volume, whereas in the other FISH-positive cells the signal was a bright

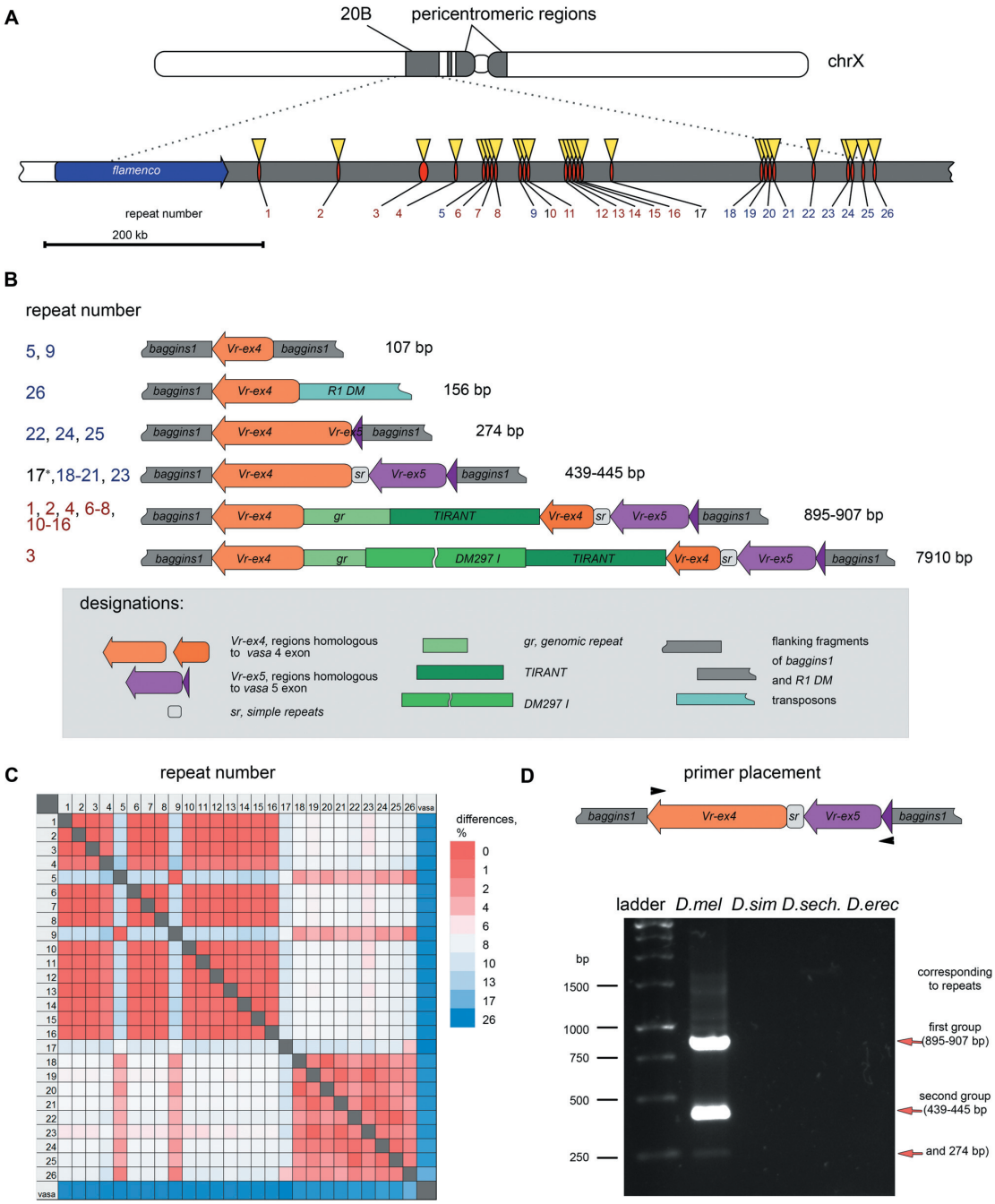

Figure 1. Distribution and structure of *AT-chX* repeats in the *Drosophila melanogaster* genome. (**A**) Localization of *AT-chX* repeats on the X chromosome of the *dm6* genome assembly. piRNA cluster *flamenco* is located 28-kb upstream of *AT-chX* repeat #1. See Supplementary Table S2 for genomic coordinates of the repeats. (**B**) Structures of the *AT-chX* repeats. Repeat numbers are indicated on the left. The lengths of repeats excluding flanking transposon sequences are indicated on the right. Similar sequences are presented as solid bars of the same color (as indicated in the key at the bottom of the panel). The *Vr-ex4* sequences (orange) are homologous to the fourth *vasa* exon; *Vr-ex5* sequences (violet) are homologous to the fifth *vasa* exon. Arrows indicate orientation of exons in *vasa* gene. Note that *Vr-ex4 and Vr-ex5* are arranged in the repeats in the reverse order relative to the corresponding exons in *vasa* gene. Internal insertions of transposons and a genomic repeat sequence of unknown origin (*gr*, up to 156 bp) are designated by green color. Short simple repeats $(TCAATGT)_n$ (21–35 bp) that connect *Vr-ex4 and Vr-ex5* are designated as *sr* (light grey boxes). As a rule, the *AT-chX* repeats are flanked by *baggins1* fragments (gray bars). The asterisk (*) indicates that repeat #17 is flanked upstream by *Stalker2* fragment and downstream by *baggins1*. (**C**) Heat map showing pairwise comparison of the *AT-chX* repeat sequences (see Supplementary Figure S1 for multiple alignments). The number of mismatches (substitutions and indels) between individual *AT-chX* repeats and *D. melanogaster vasa* mRNA is shown normalized for length. The *AT-chX* repeats form two distinct groups. The first group contains the repeats ##1–4, 6–8 and 10–16. The second group includes the repeats ##18–26, and shorter repeats #5 and #9. Repeat #17 is not included in either group because it is strongly disrupted (Supplementary Table S2 and Supplementary Figure S1). The first group numbers are presented in dark red color and the second group numbers in dark blue in (A) and (B) panels. (**D**) PCR analysis of *AT-chX* repeats in the genomes of different *Drosophila* species. The genome of *D. melanogaster* (*Oregon* strain) contains *AT-chX* repeats with the lengths of 895–907, 439–445 and 274 bp (red arrows). PCR analysis of genomic DNA from *Drosophila simulans* (w.501), *Drosophila sechellia* and *Drosophila erecta* did not reveal PCR fragments corresponding to the repeats. Positions of the primers are indicated by black arrowheads on the scheme above the gel image.

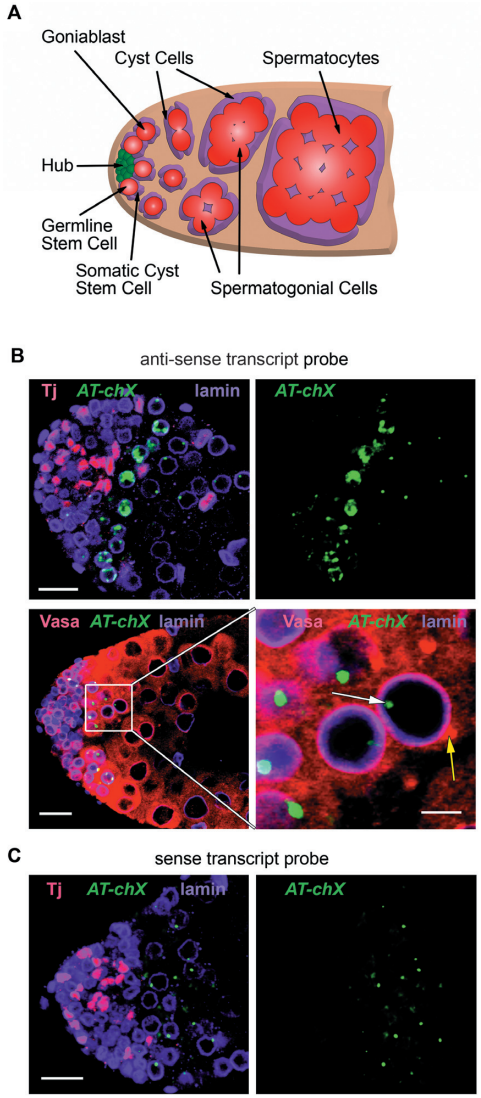

Figure 2. Expression of *AT-chX* transcripts in the testes of *Drosophila melanogaster*. (**A**) Representation of early stages of spermatogenesis in *Drosophila*. Germline stem cells (GSC) (red balls) and cyst stem cells (violet) are located adjacent to the hub structure (green balls) at the apical tip (left). The daughter of the GSC, a goniablast (red), is encapsulated by two somatic cyst cells (violet) and undergoes four mitotic divisions to generate cysts of 2, 4, 8 and finally 16 spermatogonia. The 16-cell cyst immediately starts to differentiate as cyst of spermatocytes. Spermatocytes undergo intensive growth and then enter meiosis (not shown). (**B**) RNA FISH of positive-strand *AT-chX* transcripts (antisense relative to *vasa* mRNA) in the testes of young *yw* males. Antisense *AT-chX* transcripts (green) are accumulated in the nuclei of early spermatocytes. Single internal confocal slices of an immunostained whole-mount testis preparation are shown. Testes were simultaneously immunostained with anti-Tj (red) and anti-lamin (blue) antibodies (top images) or anti-Vasa (red) and anti-lamin (blue) antibodies (bottom images). The lamin staining indicates nuclear membrane position. The apical tips of the testes are oriented leftward on all panels here and below. Scale bars are 20 μm except in the lower right image. The lower right image (scale bar is 5 μm) shows a magnification of the region outlined by a white box in the lower left image. White arrow indicates FISH signal, yellow arrow indicates the piNG-body (37). (**C**) RNA FISH of negative-strand *AT-chX* transcripts (sense relative to *vasa* mRNA) in the testes of young *yw* males. A single internal confocal slice is shown. Testes were immunostained with anti-Tj (red) and anti-lamin (blue) antibodies. Sense *AT-chX* transcripts (green signals) are expressed in the nuclei of spermatocytes on the same stage as antisense transcripts (B); however, their expression is weaker. Scale bar is 20 μm.

dot in the nuclei (Figure 2B). Sense transcripts always appeared as a single nuclear dot that likely corresponds to the site of nascent transcription (Figure 2C). The *AT-chX* transcripts did not co-localize with the large cytoplasmic granules known as piRNA nuage giant bodies (piNG-bodies) (37) or with small perinuclear nuage granules in spermatocytes (Figure 2B, bottom images). Taken together, these results indicate that both strands of the *AT-chX* repeats are transcribed during the early stage of spermatocyte development and that the antisense transcripts are considerably more abundant than the sense transcripts.

Generation of piRNAs from *AT-chX* repeats

Although piRNAs—those derived from the *Su(Ste)* locus—were first observed in the testes of *D. melanogaster* (18–20), the majority of subsequent studies have focused on piRNA expression in the female germline. To study generation of piRNAs in the testes in more detail, we prepared and sequenced a library of 18–29 nt RNAs isolated from the testes of *yw* males. The library contains three types of small RNAs that can be differentiated by their size: siRNAs (20–21 nt), miRNAs (21–23 nt) and piRNAs (23–29 nt) (Figure 3A, left diagram for only siRNAs and piRNAs). Similar to *Su(Ste)* small RNAs, small RNAs derived from the *AT-chX* repeats are present in the testis library in large amounts, with a minor fraction corresponding to siRNAs and a major fraction corresponding to piRNAs (Figure 3A, middle and right). *AT-chX* small RNAs are abundant and diverse: their expression is only about 2.5-fold lower than that of *Su(Ste)* small RNAs (Figure 3A). The 23–29 nt small RNAs produced from the *AT-chX* repeats have distinct signatures of piRNAs that they share with small RNAs derived from *Su(Ste)* locus. Like *Su(Ste)* piRNAs, *AT-chX* piRNAs are generated along the whole length of the repeat unit (Figure 3B). Antisense *AT-chX* piRNAs have a strong bias (87.4%) for uridine residue at the first position (1U). In contrast, sense piRNAs have no bias for 1U, but instead have a bias (68.5%) for adenine at position 10 (10A) indicating their generation through the ping-pong mechanism that is specific to the piRNA pathway (Figure 3C and see Supplementary Figure S3 for ping-pong pair examples). Similar, though less pronounced biases are present in *Su(Ste)* piRNAs indicating that ping-pong also actively participates in their biogenesis (Figure 3C). There is also pronounced bias for antisense and sense piRNA pairs whose 5′-ends overlap by 10 nt (Figure 3D and Supplementary Table S4, $z_{10} = 3.0$, overlap probability $p = 0.59$). This is another signature of the ping-pong mechanism. piRNA pairs whose 5′-ends overlap by 9 nt also exhibited some enrichment ($z_9 = 2.0$). However, in this case overlap probability value was only 0.05 (Supplementary Table S4). Analysis of piRNAs (23–29 nt) allowing no mismatches (0 mm) revealed that 46.9% of antisense *AT-chX* piRNAs mapped exclusively to *AT-chX* repeats of the second group (##18–26), whereas only 0.5% were mapped to the first group members. The remaining antisense reads were mapped to different repeats from both groups. The bulk of sense *AT-chX* piRNAs (86.6%) mapped only to repeats of the first group (##1–4, 6–8, 10–16) and 3.7%—to repeats of the second group (Supplementary Figure S4A). This suggests that transcription of sense and anti-

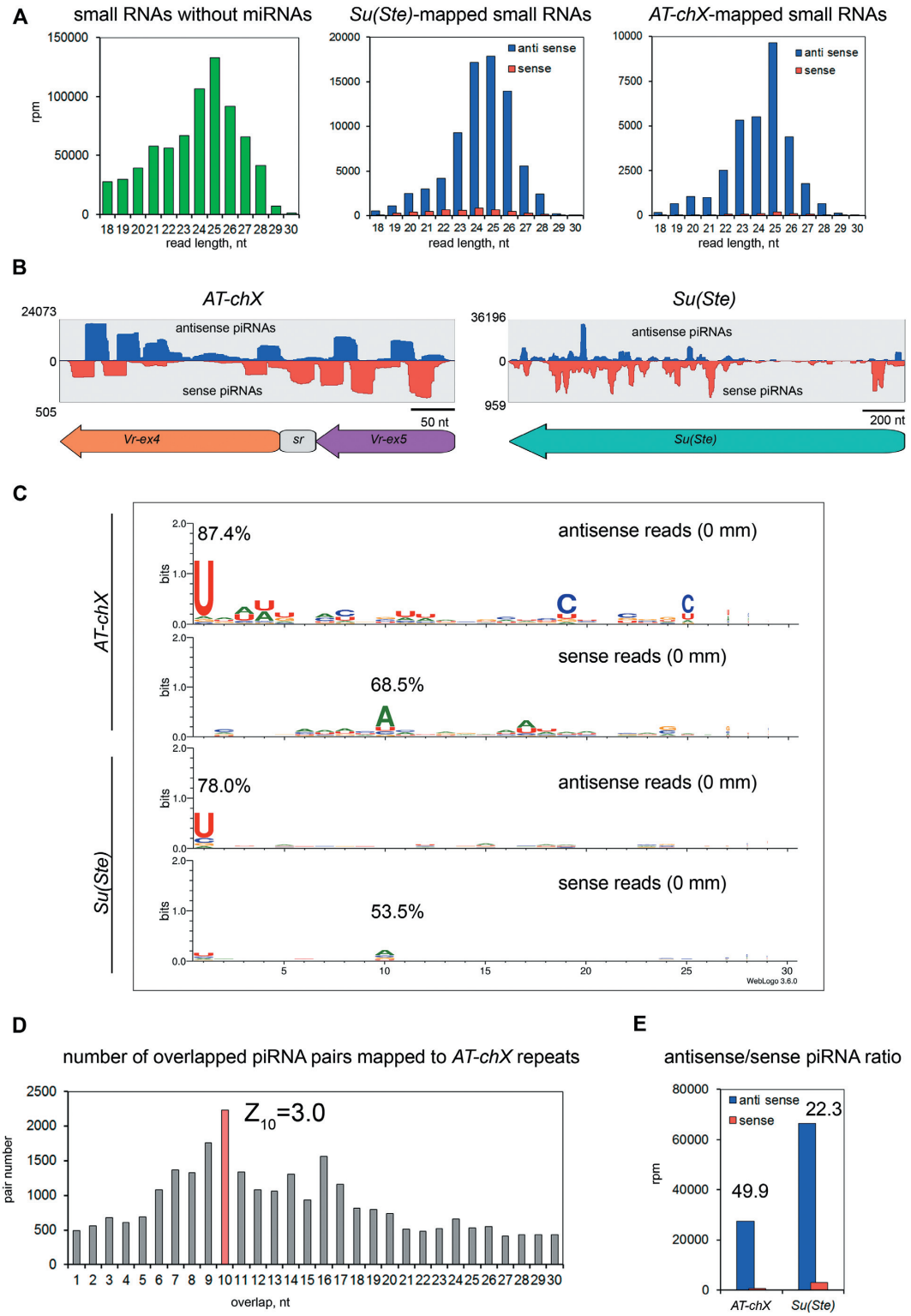

Figure 3. Comparative analyses of piRNAs mapped to *Su(Ste)* and *AT-chX* repeats. (**A**) The amount of small RNA reads (in rpm) expressed in the testes as a function of length. The left graph shows total small RNAs without annotated miRNAs, the middle and the right graphs show reads mapped to the *Su(Ste)* and *AT-chX* repeats, respectively, with no mismatches. (**B**) The distribution of *AT-chX* and *Su(Ste)* piRNAs along consensus sequences of *AT-chX* (left) and *Su(Ste)* (right) permitting 0–1 mismatches. The antisense read density graphs are shown in blue; the sense read density graphs are shown in red (the *y*-scales show read number per nucleotide position). Below the graphs are schematics of *AT-chX* (left) and *Su(Ste)* (right) consensus sequences. Arrows indicate orientation relative to *vasa* and *Stellate* mRNAs. (**C**) Nucleotide biases for *AT-chX* and *Su(Ste)* piRNAs. Percentages of reads with U1 and A10 are shown (mapped with no mismatches). (**D**) Analysis of overlap between 5′-ends of sense and antisense *AT-chX* piRNAs. The bias for 10-nt overlap indicates piRNA pairs generated through ping-pong mechanism. (**E**) Amounts of sense and antisense piRNAs derived from the *AT-chX* and *Su(Ste)* repeats sequences in rpm (no mismatches allowed). The ratios of antisense and sense piRNAs are shown above bars.

sense piRNA precursors occurs from distinct repeats. These results demonstrate that the ping-pong process is active in the biogenesis of both *AT-chX* and *Su(Ste)* piRNAs in the testes.

The piRNA pathway has no effect on the expression of the *vasa* locus in *D. melanogaster*

Using both RNA-seq and FISH, we detected a bias for expression of long antisense transcripts from the *AT-chX* repeats. The same bias was also observed for *AT-chX* piRNAs: the ratio of antisense to sense piRNAs is nearly 50-fold surpassing ∼20-fold bias observed for *Su(Ste)* piRNAs (Figure 3E). Antisense *Su(Ste)* piRNAs function in the repression of *Stellate* transcripts (18,19), while two antisense *AT-chX*-derived piRNAs were previously shown to silence *vasa* mRNA (12). However, our analysis suggests that—in contrast to *Su(Ste)* piRNAs, 26% of which can be mapped to *Stellate* sequence with zero to three mismatches thus allowing efficient targeting of *Stellate* transcripts, only a very small fraction, ∼0.85%, of antisense *AT-chX* piRNAs have zero to three mismatches to the *vasa* transcript (Supplementary Table S5). Furthermore, abundant antisense *AT-chX* piRNAs with high frequency contain mismatches to the *vasa* sequence in positions from 2 nt to 11–16 nt (Figure 4A) that were shown to be particularly important for efficient piRNA-mediated repression in *Drosophila* and mouse (8,38,39). In contrast, *Stellate*s and corresponding *Su(Ste)* piRNAs have a higher level of complementarity than *AT-chX* piRNAs do with *vasa* (Figure 4A). We also found that the targeting of *Stellate* transcripts by *Su(Ste)* piRNAs leads to the generation of secondary *Stellate*-derived piRNAs through the ping-pong mechanism with pronounced A10 bias, whereas no secondary piRNAs derived from *vasa* sequence were detected (Supplementary Figure S4B). Overall, although we found that antisense *AT-chX* piRNAs that potentially can target *vasa* mRNA were abundant in the testes, their actual ability to repress *vasa* required further testing.

To directly test the role of *AT-chX* piRNAs in the regulation of the *vasa* locus expression, we analyzed the expression of transcripts encoded on this locus in the testes of flies with mutations in *aub*, *spn-E* or *piwi* that have been shown to abolish piRNA-dependent silencing. The *aub* and *spn-E* mutations abolished repression of the *Stellate* locus by *Su(Ste)* piRNAs leading to expression of Stellate protein (18,20). The v*asa* locus of *D. melanogaster* encodes three functionally different protein-encoding transcripts: *vasa, solo* (produced by alternative splicing) and *vig* (*vasa intronic gene* encoded in the first intron of *vasa* in opposite orientation) (Figure 4B). *vasa* and *solo* have first three exons in common. The *AT-chX* piRNAs might potentially target only the fourth and a part of the fifth exons of *vasa* gene, thus, no piRNAs that match *vig* gene present. Thus, only *vasa* mRNA might be a potential target of *AT-chX* piRNAs, which therefore might participate in the regulation of the ratio of *vasa* to *solo* transcripts during a specific stage of spermatogenesis. However, in contrast to strong derepression of *Stellate* genes observed in *aub* and *spn-E* mutants, both western blot and RT-qPCR analyses detected no significant differences in mRNA and proteins encoded by the *vasa* locus in the gonads of *aub* $^{QC42/HN2}$, *spn-E*$^{1/hls3987}$ and *piwi*$^{2/3}$ flies compared to heterozygous siblings (Figure 4C and D). Immunostaining of the testes of *aub*$^{QC42/HN2}$ mutants also did not reveal repression of Vasa protein in germ cells (Figure 4E). In summary, we found no evidence for a role of the piRNA pathway in the regulation of gene expression of the *vasa* locus indicating that despite co-expression of *AT-chX* piRNAs and *vasa* mRNA in the same germ cells, the sequence similarity between them is not sufficient for effective repression.

AT-chX piRNAs repress *vasa* expression in interspecies hybrids

Unexpectedly, alignment of *vasa* sequences from the species closely related to *D. melanogaster*—*D. simulans*, *D. sechellia* and *D. mauritiana* that diverged from a common ancestor with *D. melanogaster* 2.0–5.4 million years ago (Mya) (40–43)—revealed that *vasa* sequences in these species have a high level of similarity with *AT-chX* repeats of *D. melanogaster* (90.1–90.8% identity in all three species) compared to only 76% for *vasa* of *D. melanogaster* (Supplementary Table S3 and Supplementary Figure S5). As mentioned above, we found no evidence for the presence of *AT-chX* repeats in the genomes of these species. As expected, the level of similarity between *AT-chX* repeats of *D. melanogaster* and *vasa* genes of more distantly related *Drosophila* species is lower: the identity is 77.1–78.1% in *D. yakuba* and *D. erecta* and 59.8–64.3% in *D. virilis* and *D. ananassae* (Supplementary Table S3), which have been estimated to diverge from *D. melanogaster* 8–12.8 and 44–60 Mya, respectively (41,42).

The ∼90% sequence identity between *D. melanogaster AT-chX* repeats and *vasa* mRNA sequences in the species from the *D. simulans* clade is similar to the level of identity between *Su(Ste)* repeats and *Stellate* genes in the *D. melanogaster* genome (44) and thus are expected to be sufficient for strong piRNA-dependent repression. Therefore, we decided to explore the possibility that *AT-chX* piRNAs target *vasa* mRNAs from these species in the gonads of interspecies hybrids. Viable interspecies hybrids are obtained upon crossing of *D. melanogaster* females with the *Hmr*^{1} mutation and *D. simulans* or *D. mauritiana* males (45). We observed that female progeny of crosses between *Hmr*^{1} *D. melanogaster* females and *D. simulans* or *D. mauritiana* males mostly had rudimentary ovaries with few or no germ cells (Supplementary Figure S6A and B).

The crosses between *Hmr*^{1} *D. melanogaster* females and *D. simulans* males generated only a few adult males; however, male hybrids from analogous crosses with *D. mauritiana* males were produced numerously. Importantly, the latter hybrid males have *D. melanogaster* X chromosome carrying the *AT-chX* repeats and two different alleles of the *vasa* gene, one inherited from the *D. melanogaster* mother and one from the *D. mauritiana* father. Approximately half of these hybrid males had strongly reduced testes with no Vasa-positive germ cells. However, the other half of hybrid males had testes with varying numbers of germ cells (Supplementary Figure S6C–E). Germ cell content was found to correlate with testis size. For subsequent analysis, we used a pool of hybrid testes with the maximal germ cell content

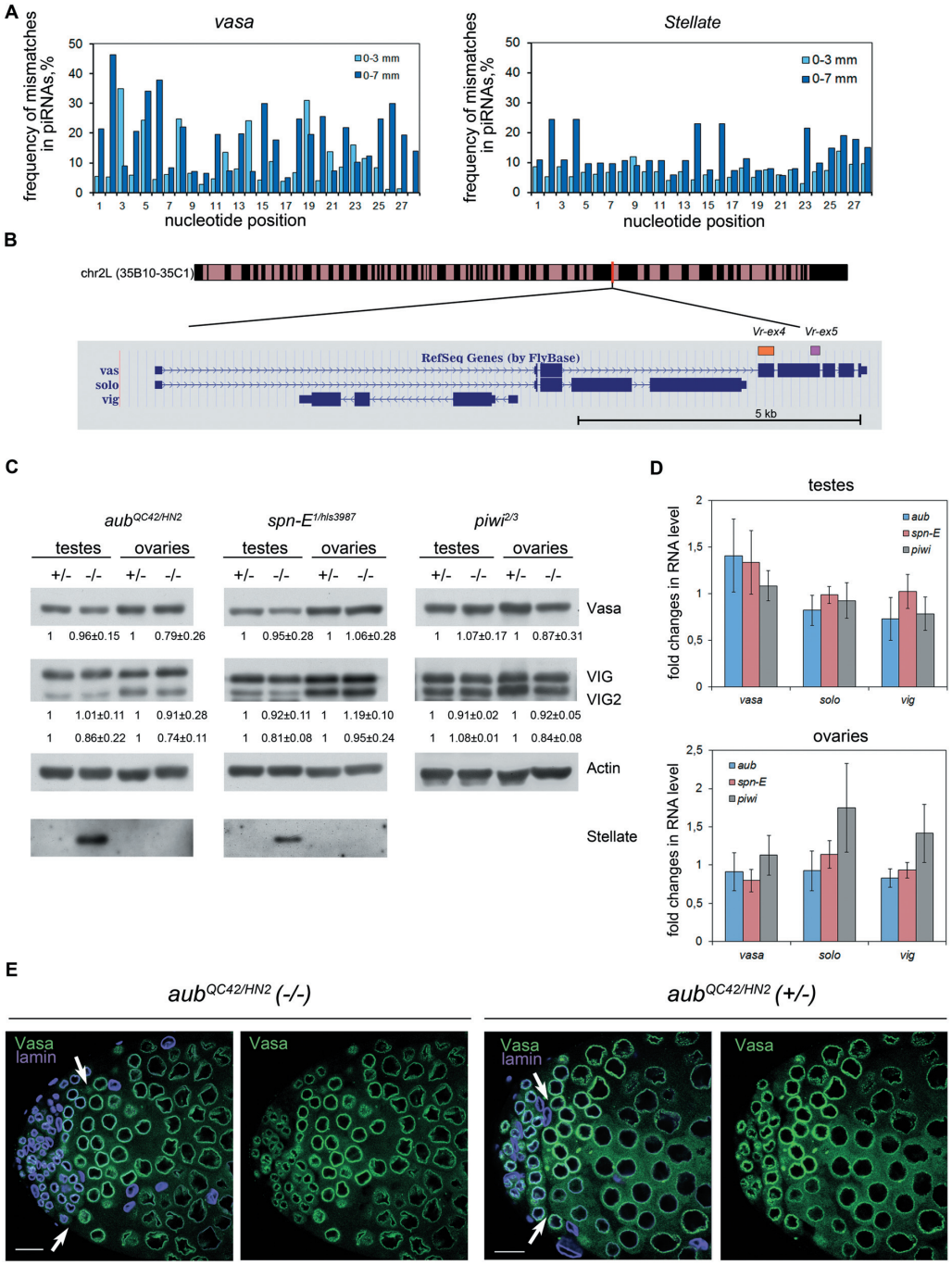

Figure 4. Analysis of piRNA-dependent regulation of *vasa* locus expression in *Drosophila melanogaster*. (**A**) Analysis of sequence identity between antisense *AT-chX* piRNAs and *vasa* mRNA (left) and between antisense *Su(Ste)* piRNAs and *Stellate* mRNAs (right). Percentages of piRNAs that have mismatches to the targets in each nucleotide position are shown for piRNA pools that mapped to target mRNAs with 0–3 mismatches (light blue bars) or 0–7 mismatches (deep blue bars). (**B**) Structure of the *vasa* locus in the genome of *D. melanogaster*. Orange and violet boxes above the fourth and fifth exons of *vasa* gene indicate relative locations of the homologous *Vr-ex4* and *Vr-ex5* sequences of the *AT-chX* repeats. (**C**) Western blot analysis of testis and ovarian lysates probed with anti-Vasa and anti-VIG/VIG2 antibodies. No changes in Vasa and VIG proteins expression in the gonads of *aub* $^{QC42/HN2}$, *spn-E*$^{1/hls3987}$ and *piwi*$^{2/3}$ mutants were found. Testes and ovaries of heterozygous siblings (+/−) were used as controls. Actin was used as a loading control. Densitometry data for Vasa, VIG and VIG2 proteins are presented under the blots. The values (obtained by using ImageJ software) were normalized to the loading control level (Actin) and then to the values obtained for the heterozygous control. Mean values and standard errors are presented for at least three independent experiments. The differences between the mutant and control preparations are insignificant in all cases ($P > 0.05$ in Student's *t*-test). (**D**) RT-qPCR analysis of transcription from the *vasa* locus in the testes and ovaries of *aub, spn-E* and *piwi* mutants. The expression levels of mRNAs were normalized to *rp49* transcripts. Fold-changes in the expression level relative to the control heterozygous siblings are shown. Error bars represent standard errors of mean. Differences between the mutant and control samples from heterozygous siblings are insignificant in all cases ($P > 0.05$). (**E**) Immunostaining of whole mount testis preparations from *aub*$^{QC42/HN2}$ heteroallelic mutant males and their heterozygous control siblings with anti-Vasa (green) and anti-lamin (blue) antibodies. Internal confocal slices are shown. Scale bars are 20 μm. White arrows indicate early spermatocyte region where transcription of *AT-chX* repeats was detected.

(>100 cells per testis). Among them, we also selected a small fraction (~1% of total amount) of the testes of wild-type size that contained a large number of Vasa-positive germ cells at different stages of maturation.

A previous report indicated that the piRNA pathway does not function properly in the ovaries of interspecies hybrids between *D. melanogaster* and *D. simulans* (46). To test if the piRNA pathway is functional in male hybrids of the cross between *D. melanogaster* and *D. mauritiana*, we first analyzed the expression of two key piRNA pathway factors, Aub and AGO3, by western blot and found that both proteins were expressed in the hybrid testes (Supplementary Figure S6F). To further analyze piRNAs in the interspecies hybrids, we next prepared and sequenced 18–29 nt small RNA libraries from the testes of parent *Hmr*^{1} *D. melanogaster* and *D. mauritiana* flies and hybrids. Analysis of the hybrid small RNA library revealed the presence of piRNA-sized 23–29 nt reads derived from various transposons indicating that the piRNA pathway is still functional in the hybrids, at least in the fraction of hybrid males that do not have drastic morphological defects in spermatogenesis (Supplementary Table S6). Importantly, analysis of piRNA pairs that overlap by 10 nt for two germline-specific transposons *HeT-A* and *TAHRE* indicated an active ping-pong piRNA biogenesis in the hybrid testes (z_{10} scores values are 4.99 and 5.10, respectively) (Supplementary Figure S6G).

To explore if targeting of *D. mauritiana vasa* gene by *AT-chX* piRNAs leads to its decreased expression in interspecies hybrids, we quantified *vasa* mRNAs of both species in the testes of the parent species and the interspecies hybrids by RT-qPCR. This analysis revealed very strong 160-fold repression of *D. mauritiana vasa* in hybrid testes, with a much milder 11.5-fold decrease in the expression of *D. melanogaster vasa* (Figure 5A). The reduced germline content observed in hybrid testes likely results in the observed general reduction in levels of germline-specific transcripts in the hybrid testes. Indeed, we found that germline-specific *aub* transcripts also decreased by the same order of magnitude in the hybrid testes (7.5- and 5.3-fold in the hybrids relative to levels in the respective parent species) (Figure 5B). The largest decrease in levels of the *D. mauritiana vasa* transcript in the hybrid testes indicates specific repression by different mechanism. Analysis of RNA-seq data confirmed the results of RT-qPCR with 14-fold repression of *D. mauritiana vasa* compared to 4-fold of *D. melanogaster vasa* in the testes of the hybrids compared to the parent species.

Next, we took advantage of the fact that both *D. melanogaster* and *D. mauritiana* Vasa are recognized by the same antibody with similar efficiency and that the proteins from the two species have slightly different electrophoretic mobilities. Western blot revealed complete disappearance of *D. mauritiana* Vasa protein in the testes of interspecies hybrids, whereas *D. melanogaster* Vasa protein was still present although in reduced amount (Figure 5C). In hybrid testes with wild-type-like morphology, only *D. melanogaster* Vasa protein was expressed and amounts were comparable to that in the parent testes (Figure 5C'). Together these results show that *vasa* genes inherited from the two parent species have unequal expression in interspecies hybrids, with expression of *D. mauritiana vasa* below the detection limit of both RT-qPCR and western analyses (Figure 5A and C-C').

Using RT-qPCR analysis, we detected the expression of *AT-chX* repeats encoded on the *D. melanogaster* X chromosome in the testes of hybrids (Figure 5A). Furthermore, *AT-chX* piRNAs were present in the hybrid testes (Supplementary Table S7) supporting the conclusion that the overall activity of the piRNA pathway is not compromised in these hybrids. As expected from the sequence analysis of the *AT-chX* repeats and *vasa* mRNAs of the parent species, a significant fraction of antisense *AT-chX* piRNAs expressed in hybrids were complementary to *D. mauritiana vasa* mRNA with zero mismatches (19.9%). In contrast, no piRNAs were complementary to *vasa* of *D. melanogaster* without mismatches (Supplementary Table S7). We found that a half of sense piRNAs (2.6 rpm) that were perfectly matched to *vasa* of *D. mauritiana* formed ping-pong pairs with antisense piRNAs (49.0 rpm) mapped to the *AT-chX* repeats with 0–3 mismatches (see Figure 5D for ping-pong pair examples). Furthermore, we detected sense piRNAs that had a pronounced A10 bias (43.5%) and that were perfectly complementary to *vasa* of *D. mauritiana* in the testes of hybrids, suggesting that these piRNAs were generated as a result of the ping-pong processing (Figure 5E). In contrast, we observed no ping-pong pairs for those sense piRNAs that were perfectly mapped to *vasa* of *D. melanogaster*, and the percentage of piRNAs with adenine at position 10 was 30.8%, close to the value expected for randomly generated sequences (Figure 5E). In sum, these results implicate piRNAs produced from the *AT-chX* repeats as a driving force for specific repression of *D. mauritiana vasa.*

Stellate derepression in the testes of interspecies hybrids

While the piRNA pathway appears to be generally active in interspecies hybrids, the Y chromosome of *D. mauritiana* that is present in hybrid males does not have the *Su(Ste)* locus. As expected, we practically did not detected *Su(Ste)* piRNAs in the testes of hybrids (Figure 6A). The absence of *Su(Ste)* piRNAs suggests that *Stellate* genes encoded on the X chromosome of *D. melanogaster* present in the hybrids might not be repressed by the piRNA pathway. The appearance in our crosses of adult hybrid males with perfectly developed testes provides a unique opportunity to study mechanisms of hybrid sterility with spatiotemporal resolution. We used this cohort of hybrid testes for further analysis to eliminate effects caused by distortion or complete collapse of spermatogenesis in hybrid males at early stages. Immunostaining showed the presence of abundant needle-like Stellate aggregates in spermatocytes of developed hybrid testes, but not in the testes of parent flies (Figure 6B–D), indicating *Stellate* derepression in the testes of hybrids. Examination of these testes revealed that spermatocytes had not progressed through meiosis, haploid spermatids were not generated and seminal vesicles were empty (Figure 6B). These effects were previously reported upon *Stellate* derepression in the testes of *D. melanogaster* due to deletion of the *Su(Ste)* locus (23,24). Thus, *Stellate* derepression caused by the lack of *Su(Ste)* piRNAs might contribute to sterility of interspecies hybrids.

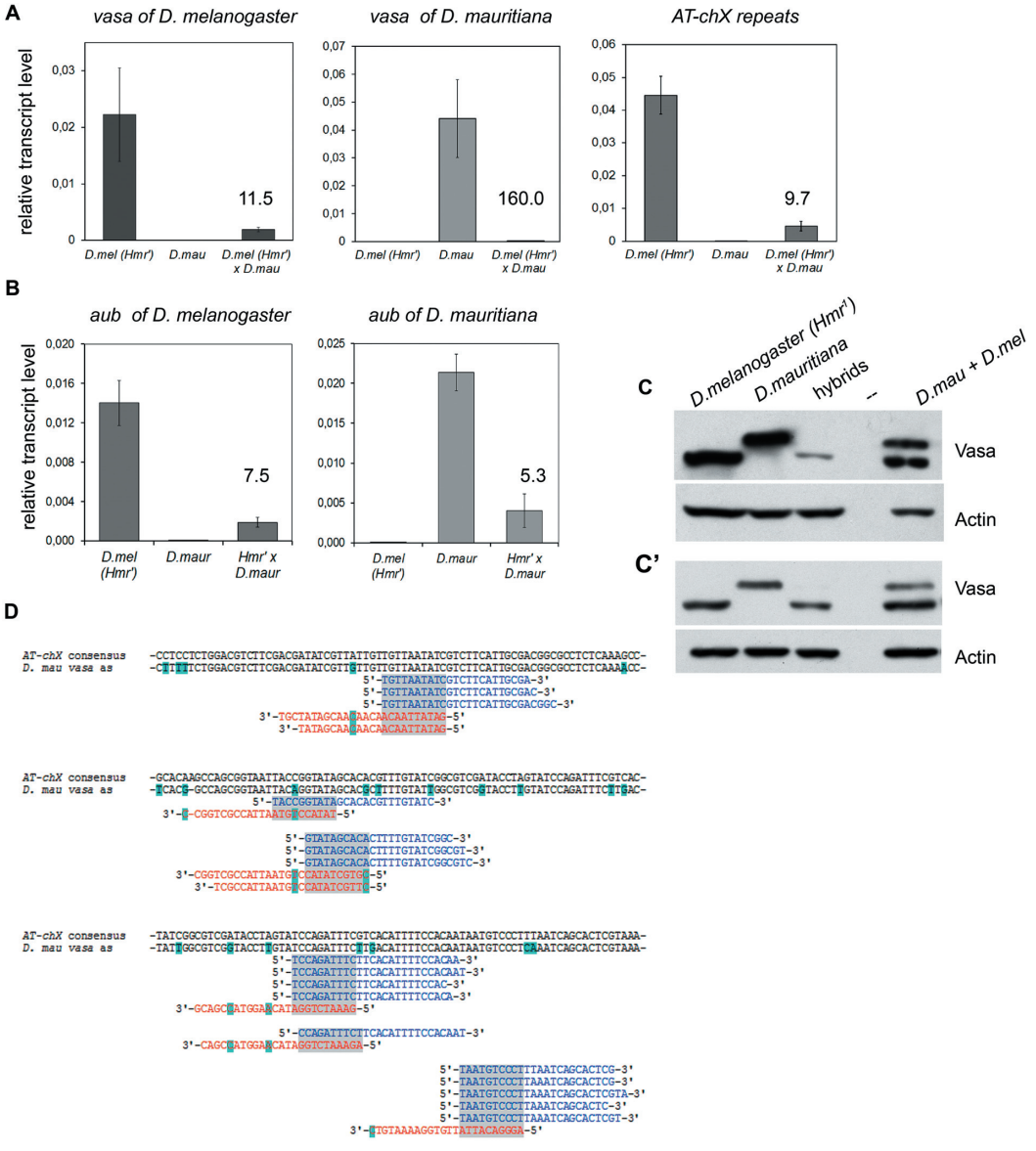

piRNAs mapped to	antisense piRNAs, U1 bias, %	sense piRNAs, A10 bias, %	ping-pong signature
AT-chX	77.8	66.3	yes
D. mel vasa	79.7	30.8	no
D. mau vasa	77.6	43.5	yes

Figure 5. Analysis of *vasa* expression in the testes of interspecies hybrids of *Drosophila melanogaster* with *Drosophila mauritiana*. (**A**) RT-qPCR analysis of transcription of *vasa* genes and *AT-chX* repeats in the testes of interspecies hybrids and parent *Drosophila* species. The level of transcripts was normalized to *rp49*. Error bars represent standard errors of mean. Fold-differences between expression in parent species and in hybrids are indicated. (**B**) RT-qPCR analysis of transcription of *aub* genes in the testes of interspecies hybrids and parent *Drosophila* species. (**C**) Western blot analysis of Vasa proteins in testis lysates from hybrids and parent *Drosophila* species. Only Vasa of *D. melanogaster* was detected in the hybrid testes. Right lane: a mixture of the same amounts of testis lysates of the parent species was loaded. (**C'**) Western blot analysis of Vasa proteins performed as in (C) using hybrid testes with wild type-like morphology. (**D**) Examples of ping-pong pairs between *AT-chX* antisense piRNAs and sense piRNAs derived from *D. mauritiana vasa* in the testes of interspecies hybrids. Sense piRNAs are marked by red, antisense piRNAs are marked by blue color. Sense piRNAs are mapped to the sequence of *D. mauritiana vasa* with zero mismatches. Only antisense reads mapped to *AT-chX* repeats with 0–1 mismatches are shown here for simplicity. The overlapped 10-nt regions of piRNAs are boxed in gray. Nucleotide substitutions in the *vasa* sequences that distinguish it from the *AT-chX* consensus are shown in cyan. (**E**) Analysis of nucleotide biases and ping-pong signatures in piRNAs expressed in the testes of interspecies hybrids. For piRNAs mapped to *AT-chX* repeats, 0–1 mismatches were allowed. For piRNAs mapped to *vasa* genes, no mismatches for sense piRNAs and 0–3 mismatches for antisense ones were allowed. Note that sense piRNAs that mapped to the sequence of *D. mauritiana vasa* (but not *D. melanogaster vasa*) without mismatches have a strong 10A bias indicating their generation by the ping-pong mechanism.

A

Libraries, % piRNAs	*Stellate* mapped piRNAs, rpm		*Su(Ste)* mapped piRNAs, rpm	
	sense	antisense	sense	antisense
Hmr[1] *D. melanogaster* testes, 26.1%	131.6	1118.0	723.3	13933.3
D. mauritiana testes, 20.1%	0.5	2.4	5.2	57.4
D. mel x *D. mau* hybrid testes, 19.4%	1.0	1.5	4.1	14.6

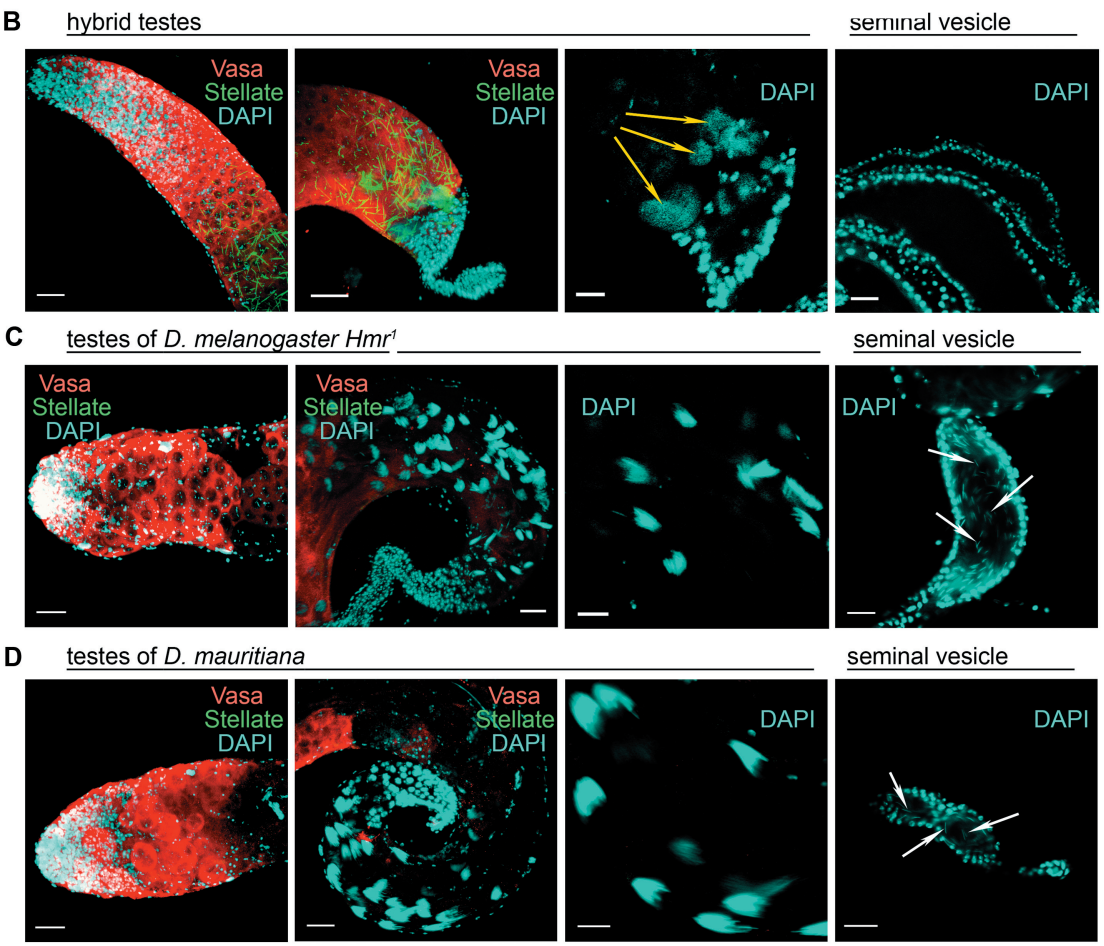

Figure 6. *Stellate* genes are derepressed in spermatocytes of hybrid testes. (**A**) Analysis of *Stellate* and *Su(Ste)* mapped piRNAs (23–29 nt) mapped with zero mismatches in the hybrid testes and testes of parent species. The percent of total piRNA reads (excluding siRNAs and miRNAs) is indicated for each library. Note that the amount of *Su(Ste)* antisense piRNAs in the hybrid testes is almost 1000-fold lower than in *Drosophila melanogaster*. (**B–D**) Immunostaining of hybrid males testes (B) and testes of parent species *D. melanogaster Hmr*[1] (C) and *Drosophila mauritiana* (D). Testes were stained with anti-Vasa (red) and anti-Stellate (green) antibodies, chromatin was stained by DAPI (cyan). 3D images are presented for apical and distal testes ends (from left two first images); single internal confocal slices are presented for seminal vesicles and enlarged fragments of distal testis ends (from right two images). Scale bars are 30 μm, for apical and distal testis ends, and seminal vesicles; 15 μm for enlarged fragments of distal testis ends (right middle image). *Stellate* genes are derepressed in spermatocytes of hybrid testes (B) and generate needle-like crystals (two left images). Spermatids are absent at the distal end of hybrid testes (left middle image). The enlarged fragment of the distal end of hybrid testis presents giant conglomerations of decondensed chromatin (B, right middle image, yellow arrows) instead of DAPI-stained heads of spermatid bundles as in the testes of parent species (C and D). This indicates severe meiotic failures in hybrid testes. Seminal vesicles of hybrids (B, right image) are empty. Seminal vesicles of *Hmr*[1] *D. melanogaster* and *D. mauritiana* males are filled by mature sperm (C and D, right images, white arrows).

DISCUSSION

We found that abnormal piRNA silencing in the male germline of interspecies hybrids of *D. melanogaster* with *D. mauritiana* causes misexpression of two different protein-coding genes, *vasa* and *Stellate*. The main function of the piRNA pathway is considered to be recognition and repression of harmful genetic elements such as transposons. Indeed, failure of the piRNA pathway causes derepression of mobile elements in the germline and somatic cells of female gonads of *D. melanogaster* (6,47). In addition to transposons, several protein-coding genes are reported as targets of piRNA-mediated regulation (11,14–18). However, the role of piRNAs in the regulation of protein-coding genes has remained an open question due to incomplete understanding of the level of sequence similarity between piRNA and its target required for successful repression. piRNAs that guide repression of transposons have a high level of sequence identity to their targets because they are transcribed from piRNA clusters, genomic regions that contain transposon sequences. In contrast, piRNAs proposed to repress host protein-coding genes have variable levels of sequence similarity to their targets and are usually generated from genomic loci that are not homologous to the putative targets (11,14). It has been even proposed that piRNAs associated with PIWI proteins may target a large number of mRNAs in a sequence-independent manner in early *Drosophila* embryos (17). Several studies have demonstrated different modes and outcomes of mRNA targeting by PIWI protein–piRNA complexes in different biological systems (14,17,39,48–51). Our results indicate that successful mRNA repression in premeiotic germ cells of *Drosophila* testes requires a high level of sequence similarity between piRNAs and their target.

We significantly expanded previous observation (12) that only two piRNAs were derived from two short *AT-chX* regions and found that multiple longer *AT-chX* repeats harbored in cytolocation 20B (Figure 1 and Supplementary Table S2) generate abundant and diverse piRNAs homologous to the sequence of *vasa* mRNA in an antisense orientation (Figure 3). Furthermore, we found that *AT-chX* piRNAs are co-expressed with *vasa* in developing spermatocytes providing an opportunity for their interaction (Figure 2). However, in contrast to previously published observation (12), our results indicate that the ∼76% sequence identity between *AT-chX* piRNAs and *vasa* was not sufficient for effective repression of *vasa* in the testes of *D. melanogaster* or interspecies hybrids (Supplementary Table S3 and Figure 4C–E). In agreement with this conclusion, the *spn-E* mutation, which disrupts piRNA biogenesis in the germline (52), did not influence *vasa* transcription or translation of *vasa* as would be expected if the *AT-chX* piRNAs mediated *vasa* repression. In contrast, strong repression was associated with generation of secondary piRNAs when the level of sequence identity between the target and piRNA is at least 90% as in the case of *Su(Ste)* piRNAs targeting *Stellate* (Supplementary Table S5) and in the case of *AT-chX* piRNAs targeting *vasa* of *D. mauritiana* across the *melanogaster–mauritiana* species barrier (Figure 5 and Supplementary Table S7). We propose that the piRNA pathway has evolved to require a high level of sequence similarity between piRNAs and their targets to prevent off-target effects.

Previous studies reported global failure of the piRNA pathway in the female germline of interspecies hybrids (46), which is hypothesized to result in global derepression of multiple piRNA target transposons. However, we found that in the male germline of interspecies hybrids piRNA biogenesis is still active and that piRNAs that target transposon transcripts are produced (Supplementary Figure S6F and G, Supplementary Table S6). This difference may result from the requirement for chromatin-associated Rhino-Deadlock-Cutoff (RDC) complex for piRNA biogenesis in the female germline (53,54); while components of this complex seem to be dispensable in males. The components of RDC complex are subject to fast evolutionary changes causing incompatibility of individual proteins from different species (55,56). Sustained activity of the piRNA pathway in the male germline of interspecies hybrids allowed us to evaluate the effects piRNAs on potential targets from two similar but distinct genomes. Deregulation of the piRNA pathway in interspecies hybrids caused abnormal expression of *vasa* and *Stellate* by two opposite mechanisms: the lack of piRNAs against *Stellate* genes caused their derepression, whereas targeting of *D. mauritiana vasa* by piRNAs generated from the *D. melanogaster* genome causes its silencing (Figures 5 and 6B–D; Supplementary Table S7; Figure 7A and B). Our results indicate that sequences of piRNAs in the germline of each species are fine-tuned to repress only correct targets and to avoid silencing of wrong targets. In the interspecies hybrids studied here, the combination of piRNAs and their target genes from the two—closely related—genomes led to failure of both mechanisms.

Both *vasa* and *Stellate* have crucial roles in spermatogenesis; however, these roles are rather opposite: the proper spermatogenesis requires *Stellate* genes that have to be repressed, while expression of *vasa* in germ cells is essential for both gonad development and gametogenesis. We found that the majority of hybrid testes had strongly reduced size and maintained just a few or no germ cells (Supplementary Figure S6C–E). We assume that *vasa* deficiency contributes to the hybrid male sterility in early stages of germ cell development (Figure 7A). In contrast to *Stellate*, *vasa* encodes a conserved DEAD-box RNA helicase that is expressed in germ cells of all Metazoa species and that is accordingly often used as a germ cell marker in evolutionary developmental biology (26). Vasa protein is enriched in the germline granules nuage, an enigmatic membraneless cytoplasmic compartment that appears to be the site of piRNA biogenesis (37,57). Though the molecular function of *vasa* is not completely understood, its expression is essential for proper germline development, gametogenesis and fertility of both sexes (27,58).

We presented here several lines of evidence that suggest that only one out of the two alleles of *vasa* is repressed in the testes of interspecies hybrids. There are comparative RT-qPCR analysis of *vasa* transcription in hybrid and parent testes, RNA-seq data and western blot analyses (Figure 5A and C-C'). This effect cannot be manifested in pure species; however, we determined it directly in the hybrid background. The specific repression in the hybrids correlates with the presence of *AT-chX* piRNAs inherited from

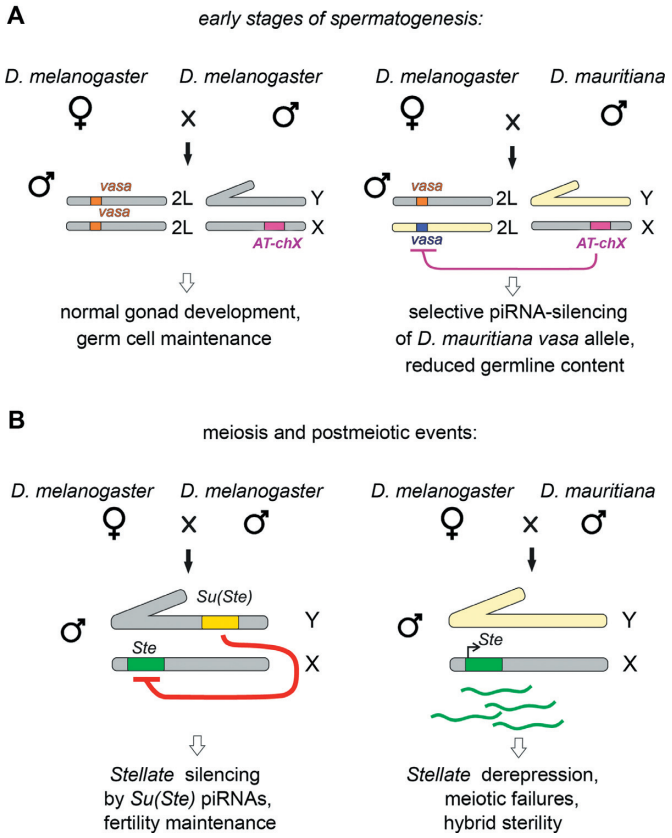

Figure 7. Models of piRNA-dependent misregulation of *Stellate* and *vasa* genes in the testes of interspecies hybrids. (**A**) Model for piRNA-dependent silencing of *D. mauritiana vasa* in the testes of interspecies hybrids. According to this model, piRNA-mediated repression of one allele of *vasa* gene in diploid hybrids might cause haploinsufficiency of *vasa* functions and might have adverse effects on germ cell development in early stages of spermatogenesis. Chromosomes of hybrids inherited from *D. melanogaster* are shown in gray and from *D. mauritiana* are shown in light yellow. (**B**) Derepession of *Stellate* genes in the testes of hybrids lacking the *Su(Ste)* locus in the genome causes meiotic failures and male hybrid sterility. Chromosome designations are as in (A).

the *D. melanogaster* genomic sequence in the hybrid testes, which are complementary to *D. mauritiana vasa*. The existence of sense piRNAs that can be perfectly mapped to *D. mauritiana* (but not *D. melanogaster*) *vasa* with 10A bias demonstrates that these piRNAs are generated by the ping-pong mechanism (Figure 5D and E).

Our comparative PCR analysis of genomic DNAs of several *D. melanogaster* strains indicates that *AT-chX* piRNAs are produced at similar levels in the testes of different strains of *D. melanogaster* (Supplementary Figure S2). However, what evolutionary forces that have allowed the *D. melanogaster* to select, fix and support *AT-chX* repeats as piRNA-producing clusters directed against an alien gene remains an unresolved issue. We found that the *AT-chX* repeats contain only regions homologous to the whole fourth exon and starting fragments of the fifth exon of *vasa* (Figure 1B) without intronic sequence between them. This feature indicates a basic attribute of retroposition. The absence of intronic sequences suggests that RNA-intermediate of an *AT-chX* precursor was inserted into the X chromosome. However, the repeats do not have other retroposition signs: they do not contain poly(A) regions and are not flanked by short direct repeated sequences. We did not find any traces of *AT-chX*-like repeats in the genome assemblies of other members of *D. melanogaster* subgroup. Thus, the origin of the *AT-chX* repeats is still a mystery.

Silencing of one allele of *vasa* gene in diploid hybrids might cause haploinsufficiency of *vasa* and adverse effects on germ cell development. It seems that repression of one *vasa* allele in hybrid testes functions upstream of *Stellate* derepression. It is known that *D. melanogaster* heterozygous *vasa* mutants are fertile (26,27). However, harmful effects of haploinsufficiency may be increased in the hybrid genetic background. *AT-chX* piRNAs are expressed in the gonads of both sexes. They appear to be stored as maternally deposited piRNAs. We propose that they could contribute to gonad developmental defects and sterility of both male and female hybrid progeny. Note that *vasa* haploinsufficiency phenotype in male and female interspecies hybrids is manifested with different penetrance (Supplementary Figure S6A–E), according to more significant requirement for *vasa* expression during oogenesis than during spermatogenesis (26,27).

Stellate genes, which are only present in *D. melanogaster* and not in other species, are normally completely repressed in the male germline. It is known that *D. melanogaster* males with mutations in piRNA pathway factors express *Stellate* in spermatocytes but not in undifferentiated germline stem cells (23,25). Abnormal expression of *Stellate* causes the appearance of abundant needle-shaped protein crystals in spermatocytes, subsequent defects in meiotic chromosome behavior and sterility (21–24). Only a small fraction of hybrid testes maintained perfect germ cell array including spermatocytes in our interspecies crosses. In these testes, the derepression of *Stellate* genes occurred with the generation of Stellate aggregates in spermatocytes and subsequent meiotic catastrophe (Figures 6B and 7B). Therefore, derepression of *Stellate* in the testes of hybrid males is likely an important factor in male hybrid sterility at the late stages of spermatogenesis.

Reproductive isolation is a necessary condition for speciation (1,59). Postzygotic reproductive isolation appears as a consequence of random accumulation of genetic differences between isolated populations of ancient precursor due to neutral selection or drift. The process of speciation results from sequential accumulation of various types of postzygotic changes, which overlap with each other and lead to a lower fitness or sterility of the hybrid progeny. Previous studies showed that interspecies hybrids have a unique genetic background that is not simply an additive combination of the two parental genomes (reviewed in (59,60)). Hybrid sterility can arise from sequence divergence that prevents chromosome paring (61,62), epistatic effects not predictable based on parental phenotypes, aberrations in gene expression, inappropriate activity of silenced genes and selfish elements (46,56), and/or asymmetric parental contributions owing to maternally inherited content (63). Our findings add misregulation of piRNA silencing, which can lead to inappropriate targeting of some genes and to the loss of legitimate repression of other genes, to the list of molecular

mechanisms that underlie reproductive isolation of closely related species.

DATA AVAILABILITY

GEO accession number for the library data is GSE120802.

SUPPLEMENTARY DATA

Supplementary Data are available at NAR Online.

ACKNOWLEDGEMENTS

We thank the Developmental Studies Hybridoma Bank for maintaining some of the antibodies used in this study. We thank M. Siomi, E. Gracheva, R. Lehmann, and D. Dodt for antibodies and O. M. Olenkina for help with fly manipulations. We thank R. Sachidanandam for help with bioinformatics analysis. The authors thank the Common Use Center of scientific equipment of the Institute of Molecular Genetics RAS, for providing the equipment.

FUNDING

Ministry of Education and Science of Russian Federation [14.W03.31.0007]. Funding for open access charge: Ministry of Education and Science of Russian Federation [14.W03.31.0007].
Conflict of interest statement. None declared.

REFERENCES

1. Coyne,J.A. and Orr,H.A. (2004) *Speciation*. Sinauer Associates, Inc., Sunderland.
2. Castillo,D.M. and Barbash,D.A. (2017) Moving speciation genetics forward: Modern techniques build on foundational studies in *Drosophila*. *Genetics*, **207**, 825–842.
3. Czech,B. and Hannon,G.J. (2016) One loop to rule them all: the Ping-Pong cycle and piRNA-Guided silencing. *Trends Biochem. Sci.*, **41**, 324–337.
4. Huang,X., Fejes Toth,K. and Aravin,A.A. (2017) piRNA biogenesis in drosophila melanogaster. *Trends Genet.*, **33**, 882–894.
5. Klattenhoff,C., Bratu,D.P., McGinnis-Schultz,N., Koppetsch,B.S., Cook,H.A. and Theurkauf,W.E. (2007) *Drosophila* rasiRNA pathway mutations disrupt embryonic axis specification through activation of an ATR/Chk2 DNA damage response. *Dev. Cell*, **12**, 45–55.
6. Malone,C.D., Brennecke,J., Dus,M., Stark,A., McCombie,W.R., Sachidanandam,R. and Hannon,G.J. (2009) Specialized piRNA pathways act in germline and somatic tissues of the *Drosophila* ovary. *Cell* **137**, 522–535.
7. Brennecke,J., Aravin,A.A., Stark,A., Dus,M., Kellis,M., Sachidanandam,R. and Hannon,G.J. (2007) Discrete small RNA-generating loci as master regulators of transposon activity in *Drosophila*. *Cell*, **128**, 1089–1103.
8. Mohn,F., Handler,D. and Brennecke,J. (2015) Noncoding RNA. piRNA-guided slicing specifies transcripts for Zucchini-dependent, phased piRNA biogenesis. *Science*, **348**, 812–817.
9. Han,B.W., Wang,W., Li,C., Weng,Z. and Zamore,P.D. (2015) Noncoding RNA. piRNA-guided transposon cleavage initiates Zucchini-dependent, phased piRNA production. *Science*, **348**, 817–821.
10. Gunawardane,L.S., Saito,K., Nishida,K.M., Miyoshi,K., Kawamura,Y., Nagami,T., Siomi,H. and Siomi,M.C. (2007) A slicer-mediated mechanism for repeat-associated siRNA 5′ end formation in *Drosophila*. *Science*, **315**, 1587–1590.
11. Saito,K., Inagaki,S., Mituyama,T., Kawamura,Y., Ono,Y., Sakota,E, Kotani,H., Asai,K., Siomi,H. and Siomi,M.C. (2009) A regulatory circuit for piwi by the large Maf gene *traffic jam* in *Drosophila*. *Nature*, **461**, 1296–1299.
12. Nishida,K.M., Saito,K., Mori,T., Kawamura,Y., Nagami-Okada,T., Inagaki,S., Siomi,H. and Siomi,M.C. (2007) Gene silencing mechanisms mediated by Aubergine piRNA complexes in *Drosophila* male gonad. *RNA*, **13**, 1911–1922.
13. Nagao,A., Mituyama,T., Huang,H., Chen,D., Siomi,M.C. and Siomi,H. (2010) Biogenesis pathways of piRNAs loaded onto AGO3 in the *Drosophila* testis. *RNA*, **16**, 2503–2515.
14. Barckmann,B., Pierson,S., Dufourt,J., Papin,C., Armenise,C., Port,F., Grentzinger,T., Chambeyron,S., Baronian,G., Desvignes,J.P. *et al.* (2015) Aubergine iCLIP reveals piRNA-Dependent decay of mRNAs involved in germ cell development in the early embryo. *Cell Rep.*, **12**, 1205–1216.
15. Rojas-Rios,P., Chartier,A., Pierson,S. and Simonelig,M. (2017) Aubergine and piRNAs promote germline stem cell self-renewal by repressing the proto-oncogene Cbl. *EMBO J.*, **36**, 3194–3211.
16. Klein,J.D., Qu,C., Yang,X., Fan,Y., Tang,C. and Peng,J.C. (2016) *c-Fos* repression by piwi regulates *Drosophila* ovarian germline formation and tissue morphogenesis. *PLoS Genet.*, **12**, e1006281.
17. Vourekas,A., Alexiou,P., Vrettos,N., Maragkakis,M. and Mourelatos,Z. (2016) Sequence-dependent but not sequence-specific piRNA adhesion traps mRNAs to the germ plasm. *Nature*, **531**, 390–394.
18. Aravin,A.A., Naumova,N.M., Tulin,A.V., Vagin,V.V., Rozovsky,Y.M. and Gvozdev,V.A. (2001) Double-stranded RNA-mediated silencing of genomic tandem repeats and transposable elements in the *D. melanogaster* germline. *Curr. Biol.*, **11**, 1017–1027.
19. Aravin,A.A., Klenov,M.S., Vagin,V.V., Bantignies,F., Cavalli,G. and Gvozdev,V.A. (2004) Dissection of a natural RNA silencing process in the *Drosophila melanogaster* germ line. *Mol. Cell Biol.*, **24**, 6742–6750.
20. Vagin,V.V., Sigova,A., Li,C., Seitz,H., Gvozdev,V. and Zamore,P.D. (2006) A distinct small RNA pathway silences selfish genetic elements in the germline. *Science*, **313**, 320–324.
21. Hardy,R.W., Lindsley,D.L., Livak,K.J., Lewis,B., Siversten,A.L., Joslyn,G.L., Edwards,J. and Bonaccorsi,S. (1984) Cytogenetic analysis of a segment of the Y chromosome of *Drosophila melanogaster*. *Genetics*, **107**, 591–610.
22. Livak,K.J. (1990) Detailed structure of the *Drosophila melanogaster stellate* genes and their transcripts. *Genetics*, **124**, 303–316.
23. Bozzetti,M.P., Massari,S., Finelli,P., Meggio,F., Pinna,L.A., Boldyreff,B., Issinger,O.G, Palumbo,G., Ciriaco,C., Bonaccorsi,S. *et al.* (1995) The Ste locus, a component of the parasitic *cry-Ste* system of *Drosophila melanogaster*, encodes a protein that forms crystals in primary spermatocytes and mimics properties of the beta subunit of casein kinase 2. *Proc. Natl. Acad. Sci. U.S.A.*, **92**, 6067–6071.
24. Palumbo,G., Bonaccorsi,S., Robbins,L.G. and Pimpinelli,S. (1994) Genetic analysis of *Stellate* elements of *Drosophila melanogaster*. *Genetics*, **138**, 1181–1197.
25. Egorova,K.S., Olenkina,O.M., Kibanov,M.V., Kalmykova,A.I., Gvozdev,V.A. and Olenina,L.V. (2009) Genetically derepressed nucleoplasmic stellate protein in spermatocytes of *D. melanogaster* interacts with the catalytic subunit of protein kinase 2 and carries histone-like lysine-methylated mark. *J. Mol. Biol.*, **389**, 895–906.
26. Lasko,P. (2013) The DEAD-box helicase Vasa: evidence for a multiplicity of functions in RNA processes and developmental biology. *Biochim. Biophys. Acta*, **1829**, 810–816.
27. Dehghani,M. and Lasko,P. (2017) Multiple functions of the DEAD-Box helicase vasa in *Drosophila* oogenesis. *Results Probl. Cell Differ.*, **63**, 127–147.
28. Nolte,V., Pandey,R.V., Kofler,R. and Schlötterer,C. (2013) Genome-wide patterns of natural variation reveal strong selective sweeps and ongoing genomic conflict in *Drosophila mauritiana*. *Genome Res.*, **23**, 99–110.
29. Aravin,A.A., Sachidanandam,R., Bourc'his,D., Schaefer,C., Pezic,D., Toth,K.F., Bestor,T. and Hannon,G.J. (2008) A piRNA pathway primed by individual transposons is linked to de novo DNA methylation in mice. *Mol. Cell*, **31**, 785–799.
30. Crooks,G.E., Hon,G., Chandonia,J.M. and Brenner,S.E.2004. WebLogo: a sequence logo generator. *Genome Res.*, **14**, 1188–1190.
31. Antoniewski,C. (2014) Computing siRNA and piRNA overlap signatures. *Methods Mol. Biol.*, **1173**, 135–146.
32. Quinlan,A.R. and Hall,I.M. (2010) BEDTools: a flexible suite of utilities for comparing genomic features. *Bioinformatics*, **26**, 841–842.

33. Li,H., Handsaker,B., Wysoker,A., Fennell,T., Ruan,J., Homer,N., Marth,G., Abecasis,G., Durbin,R. and 1000 Genome Project Data Processing Subgroup (2009) The Sequence Alignment/Map format and SAMtools. *Bioinformatics*, **25**, 2078–2079.
34. Kibanov,M.V., Kotov,A.A. and Olenina,L.V. (2013) Multicolor fluorescence imaging of whole-mount *Drosophila* testes for studying spermatogenesis. *Anal. Biochem.*, **436**, 55–64.
35. Li,M.A., Alls,J.D., Avancini,R.M., Koo,K. and Godt,D. (2003) The large Maf factor Traffic Jam controls gonad morphogenesis in *Drosophila*. *Nat. Cell Biol.*, **5**, 994–1000.
36. Gracheva,E., Dus,M. and Elgin,S.C. (2009) Drosophila RISC component VIG and its homolog Vig2 impact heterochromatin formation. *PLoS One*, **4**, e6182.
37. Kibanov,M.V., Egorova,K.S., Ryazansky,S.S., Sokolova,O.A., Kotov,A.A., Olenkina,O.M., Stolyarenko,A.D., Gvozdev,V.A. and Olenina,L.V. (2011) A novel organelle, the piNG-body, in the nuage of *Drosophila* male germ cells is associated with piRNA-mediated gene silencing. *Mol. Biol. Cell*, **22**, 3410–3419.
38. Wang,W., Yoshikawa,M., Han,B.W., Izumi,N., Tomari,Y., Weng,Z. and Zamore,P.D. (2014) The initial uridine of primary piRNAs does not create the tenth adenine that Is the hallmark of secondary piRNAs. *Mol. Cell*, **56**, 708–716.
39. Goh,W.S., Falciatori,I, Tam,O.H., Burgess,R., Meikar,O., Kotaja,N., Hammell,M. and Hannon,G.J. (2015) piRNA-directed cleavage of meiotic transcripts regulates spermatogenesis. *Genes Dev.*, **29**, 1032–1044.
40. Lachaise,D., Cariou,M.L., David,J.R., Lemeunier,F., Tsacas,L. and Ashburner,M. (1988) Historical biogeography of the *Drosophila-Melanogaster* species subgroup. *Evol. Biol.*, **22**, 159–225.
41. Russo,C.A., Takezaki,N. and Nei,M. (1995) Molecular phylogeny and divergence times of drosophilid species. *Mol. Biol. Evol.*, **12**, 391–404.
42. Tamura,K., Subramanian,S. and Kumar,S. (2004) Temporal patterns of fruit fly (*Drosophila*) evolution revealed by mutation clocks. *Mol. Biol. Evol.*, **21**, 36–44.
43. Dean,M.D. and Ballard,J.W. (2004) Linking phylogenetics with population genetics to reconstruct the geographic origin of a species. *Mol. Phylogenet. Evol.*, **32**, 998–1009.
44. Kogan,G.L., Epstein,V.N., Aravin,A.A. and Gvozdev,V.A. (2000) Molecular evolution of two paralogous tandemly repeated heterochromatic gene clusters linked to the X and Y chromosomes of *Drosophila melanogaster*. *Mol. Biol. Evol.,* **17**, 697–702.
45. Barbash,D.A. and Ashburner,M. (2003) A novel system of fertility rescue in *Drosophila* hybrids reveals a link between hybrid lethality and female sterility. *Genetics*, **163**, 217–226.
46. Kelleher,E.S., Edelman,N.B. and Barbash,D.A. (2012) *Drosophila* interspecific hybrids phenocopy piRNA-pathway mutants. *PLoS Biol.*, **10**, e1001428.
47. Li,C., Vagin,V.V., Lee,S., Xu,J., Ma,S., Xi,H., Seitz,H., Horwich,M.D., Syrzycka,M., Honda,B.M. *et al.* (2009) Collapse of germline piRNAs in the absence of Argonaute3 reveals somatic piRNAs in flies. *Cell*, **137**, 509–521.
48. Rouget,C., Papin,C., Boureux,A., Meunier,A.C., Franco,B., Robine,N., Lai,E.C., Pelisson,A. and Simonelig,M. (2010) Maternal mRNA deadenylation and decay by the piRNA pathway in the early *Drosophila* embryo. *Nature*, **467**, 1128–1132.
49. Gou,L.T., Dai,P., Yang,J.H., Xue,Y., Hu,Y.P., Zhou,Y., Kang,J.Y., Wang,X., Li,H., Hua,M.M. *et al.* (2014) Pachytene piRNAs instruct massive mRNA elimination during late spermiogenesis. *Cell Res.*, **24**, 680–700.
50. Dufourt,J., Bontonou,G., Chartier,A., Jahan,C., Meunier,A.C., Pierson,S., Harrison,P.F., Papin,C., Beilharz,T.H. and Simonelig,M. (2017) piRNAs and Aubergine cooperate with Wispy poly(A) polymerase to stabilize mRNAs in the germ plasm. *Nat. Commun.*, **8**, 1305.
51. Rojas-Ríos,P. and Simonelig,M. (2018) piRNAs and PIWI proteins: regulators of gene expression in development and stem cells. *Development*, **145**, dev161786.
52. Ryazansky,S.S., Kotov,A.A., Kibanov,M.V., Akulenko,N.V., Korbut,A.P., Lavrov,S.A., Gvozdev,V.A. and Olenina,L.V. (2016) RNA helicase Spn-E is required to maintain Aub and AGO3 protein levels for piRNA silencing in the germline of *Drosophila*. *Eur. J. Cell Biol.*, **95**, 311–322.
53. Le Thomas,A., Stuwe,E., Li,S., Du,J., Marinov,G., Rozhkov,N., Chen,Y.C., Luo,Y., Sachidanandam,R., Toth,K.F. *et al.* (2014) Transgenerationally inherited piRNAs trigger piRNA biogenesis by changing the chromatin of piRNA clusters and inducing precursor processing. *Genes Dev.*, **28**, 1667–1680.
54. Chen,Y.A., Stuwe,E., Luo,Y., Ninova,M., Le Thomas,A., Rozhavskaya,E., Li,S., Vempati,S., Laver,J.D., Patel,D.J. *et al.* (2016) Cutoff suppresses RNA Polymerase II termination to ensure expression of piRNA precursors. *Mol. Cell*, **63**, 97–109.
55. Simkin,A., Wong,A., Poh,Y.P., Theurkauf,W.E. and Jensen,J.D. (2013) Recurrent and recent selective sweeps in the piRNA pathway. *Evolution*, **67**, 1081–1090.
56. Parhad,S.S., Tu,S., Weng,Z. and Theurkauf,W.E. (2017) Adaptive evolution leads to Cross-Species incompatibility in the piRNA transposon silencing machinery. *Dev. Cell*, **43**, 60–70.
57. Lim,A.K. and Kai,T. (2007) Unique germ-line organelle, nuage, functions to repress selfish genetic elements in *Drosophila melanogaster*. *Proc. Natl. Acad. Sci. U.S.A.*, **104**, 6714–6719.
58. Kotov,A.A., Akulenko,N.V., Kibanov,M.V. and Olenina,L.V. (2014) Dead-box RNA helicases in animal gametogenesis. *Mol. Biol.*, **48**, 22–35.
59. Maheshwari,S. and Barbash,D.A. (2011) The genetics of hybrid incompatibilities. *Annu. Rev. Genet.*, **45**, 331–355.
60. Michalak,P. (2009) Epigenetic, transposon and small RNA determinants of hybrid dysfunctions. *Heredity* , **102**, 45–50.
61. Naveira,H. and Fondevila,A. (1991) The evolutionary history of *Drosophila buzzatii*. XXI. Cumulative action of multiple sterility factors on spermatogenesis in hybrids of *D. buzzatii* and *D. koepferae*. *Heredity*, **67**, 57–72.
62. Ferree,P.M. and Barbash,D.A. (2009) Species-specific heterochromatin prevents mitotic chromosome segregation to cause hybrid lethality in *Drosophila*. *PLoS Biol.*, **7**, e1000234.
63. Ferree,P.M. and Barbash,D.A. (2007) Distorted sex ratios: a window into RNAi-mediated silencing. *PLoS Biol.*, **5**, e303.